Environmental and Experimental Botany 217 (2024) 105563

Contents lists available at ScienceDirect

Environmental and Experimental Botany

journal homepage: www.elsevier.com/locate/envexpbot

Modulation of morpho-physiological attributes and in situ analysis of secondary metabolites using Raman spectroscopy in response to red and blue light exposure in *Artemisia annua*

Nidhi Rai [a,1], Sabitri Kumari [a], Sneha Singh [a], Pajeb Saha [a], Adarsh Kumar Pandey [b], Shashi Pandey-Rai [a,*,2]

[a] *Laboratory of Morphogenesis, Centre of Advance Study in Botany, Department of Botany, Institute of Science, Banaras Hindu University, Varanasi 221005, Uttar Pradesh, India*

[b] *Sophisticated Analytical and Technical Help Institute, Banaras Hindu University, Varanasi 221005, Uttar Pradesh, India*

ARTICLE INFO

Keywords:
LEDs light
Secondary metabolites
Artemisia annua
Flavonoids
Phenolics
Antioxidant enzymes

ABSTRACT

Differential light conditions, such as variations in photoperiod, light quality, and light intensity, play a crucial role as external factors that can influence plant morphogenesis and secondary metabolism. However, there is still a lack of understanding of how *Artemisia annua* responds to monochromatic and dichromatic light regimes in terms of the different physiological mechanisms that control plant growth and secondary metabolite production. Therefore, the primary aim of this study was to investigate and assess the various physiological parameters, biochemical analysis, and molecular aspects in detail. Therefore, the plantlets were exposed to LED lighting such as monochromatic red light (R), monochromatic blue light (B), white light (W), and a combination of red and blue light (RB, 1:1) at a PPFD (photosynthetic photon flux density) of 200 mol. m^{-2}. s^{-1} for 10 days. Our results indicate that exposure to RB light resulted in an immense increase in ROS accumulation, flavonoids, lignin, and artemisinin by 4.7-fold, 44%, and 53.4%, respectively, in contrast to W light. Whereas blue light led to increments of 160.2% in phenolic and 107.9% in anthocyanin content. RB and B light also influence the parameters of chlorophyll fluorescence, as well as leaf area, stomatal density, trichome size, antioxidant enzyme activity, and the production of more secondary metabolites to combat oxidative stress. Real-time PCR analysis of biosynthetic pathway-associated genes HMGR, DXR, DXS, FPS, ADS, CYP71AVI, DBR2, ALDH1, and flavonoid key biosynthesis pathway genes PAL, C4H, 4CL, CHS, and F3′H showed the highest increment under RB, light followed by B and R light exposure. Further, RB LED light has significant potential for enhancing natural bio-active compounds as revealed by Raman spectroscopy, such as camphor, limonene, terpene-4-ol, α pinene, 1,8-cineole, β-caryophyllene, artemisinin, kaempferol, luteolin, rutin, and caffeic acid in *A. annua*. Taken together, red and blue LEDs can serve as significant elicitors for the production of commercially important metabolites.

Abbreviations: LED, Light-emitting diodes; W, White light; R, Red light; B, Blue light; RB, Red +blue light in 1:1 ratio; PPFD, Photosynthetic photon flux density; Fo, Minimum fluorescence; Fm, Maximum fluorescence; qP, Photochemical quenching; ETR, Electron transport rate; ϕPSII, Relative quantum efficiency of PSII photochemistry; NPQ, Non-photochemical quenching; Fv, Variable fluorescence; Fv/Fm, Variable fluorescence to the maximum fluorescence ratio; SOD, Superoxide dismutase; POD, Peroxidase; GR, Glutathione reductase; CAT, Catalase; ROS, Reactive oxygen species; NBT, Nitroblue tetrazolium staining; DAB, 3,3-diaminobenzidine; HMGR, 3-Hydroxyl-3-methyglutaryl CoA reductase; MK, Mevalonate kinase; MPK, Mevalonate-5-phosphate kinase; MPDC, Mevalonate phosphate decarboxylase; DXS, 1-Deoxy-D-xylulose-5-phosphate synthase; DXR, 1-Deoxy-D-xylulose-5-phosphate reductoisomerase; IPPi, Isopentenyl pyrophosphate isomerase; FPS, Fernasyl diphosphate synthase; GGPRS, Geranylgeranyl pyrophosphate synthase; ALDH1, Aldehyde dehydrogenase; DBR2, Double bond reductase2; ADS, Amorpha-4,11-diene synthase; CYP71AV1, CytochromeP450dependent monooxygenase/hydroxylase; PAL, Phenylalanine ammonia-lyase; C4H, Cinnamate-4-hydroxylase; 4CL, 4-coumarate CoA ligase; CHS, Chalcone synthase; F3′H, Flavonoid-3′-hydroxylase; FNR, Ferredoxin NADP reductase; FNS, Flavone synthase; FLS, Flavonol synthase; DFR, Dihydroflavonol-4 reductase; CMS, 4-diphosphocytidyl-2-C-methyl-D-erythritol synthase; MCS, 2-C-methyl-D- erythritol 2,4-cyclodiphosphate synthase; HDS, 1-hydroxy-2-methyl-2-(*E*)-butenyl4-diphosphate synthase; HPLC, High-Performance Liquid Chromatography; GC-MS, Gas Chromatography-Mass Spectrometry; SEM, Scanning electron microscope.

* Corresponding author.
E-mail addresses: shashi.bhubotany@gmail.com, pshashi@bhu.ac.in (S. Pandey-Rai).
[1] 0000-0002-9543-7680
[2] 0000-0002-6998-1594

https://doi.org/10.1016/j.envexpbot.2023.105563
Received 14 September 2023; Received in revised form 11 November 2023; Accepted 11 November 2023
Available online 17 November 2023

1. Introduction

Light serves as an indispensable and essential signal that plants utilize for growth and developmental processes and as the main energy source for photosynthesis. The signals are detected by plants via various photoreceptors and are responsible for specific downstream cascades for a variety of physiological responses (Casal, 2013; Huché-Thélier et al., 2016). It has been reported that not only the intensity but also the spectral quality of light plays a significant role in regulating physiological and biochemical changes in plants (Neff et al., 2000). Plants respond differently to various types of light. The wavelengths of blue (B) and red (R) lights are highly efficient for the process of plant photosynthesis. This is due to the prevalence of wavelengths ranging from 400 to 500 nm for B light and 600–700 nm for R light, which are primarily absorbed by photosynthetic pigments (Z. Yang et al., 2017). The relevance of growing plants under monochromatic red (R) or blue (B) light is reliant upon the specific objectives and demands of plant growth and development. Both red and blue light wavelengths are crucial for the optimal growth and development of plants, as they serve distinct functions in many physiological processes. The specific combination of red and blue light, along with the length and intensity of each, can be modified to suit the requirements of different plant species and growth phases. Furthermore, specific advantages can be seen in plants exposed to B and R light, either individually or in combination, each contributing to optimal growth and development (Olle and Viršile, 2013). B light is perceived by phototropin, which regulates phototropism, stomatal opening, and chloroplast movement. Cryptochromes are also activated by B light and are responsible for the blooming of flowers, etiolation, stomatal opening, and elongation of primary roots (Apoorva. et al., 2021; Galvão and Fankhauser, 2015). B light-grown plants exhibited maximum photosynthetic activity in contrast to R light-exposed plants. The increment was observed in chlorophyll a/b ratios, elevated electron transport systems, enhanced Rubisco activity, and upregulation of gene expression related to the C3 cycle (X. Yang et al., 2018). Additionally, far-red and R lights are sensed via phytochromes that play a pivotal role in germination, stomatal development, and the blooming of flowers.

Numerous experiments have been performed on several plant species, showcasing the benefits of the addition of LED lighting (light-emitting diodes) under in-vitro conditions (de Hsie et al., 2019). Today's LEDs are gaining ground over conventional lighting such as incandescent, fluorescent, and metal halide due to their low thermal output, longer lifespan, energy efficiency, and many other benefits (Kurilčik et al., 2008; Monostori et al., 2018). It has been reported that certain light spectra are capable of stimulating the bioactive compounds in medicinal plants that have pharmaceutical attributes. Recently, there has been an increment in the utilization of various light qualities for the improvement of bioactive compounds of therapeutic relevance under restrained environments, such as in-vitro growth, greenhouses, plant factories, and hydroponic cultivation (C.-C. Chen et al., 2020). Additionally, plants that were grown in an in-vitro environment under varying light regimes showed enhanced growth, elevated antioxidant enzymes, and improved secondary metabolite production. Goins et al. (2001) reported enhanced biomass production in radish and lettuce under R light exposure. Similarly, in *Ajuga bracteosa,* there was an increase in secondary metabolite accumulation under differential light-quality treatments (Ali et al., 2019). These findings highlight the potential of changing the quality of light to maximize the growth of plants and the production of secondary metabolites under in-vitro culture systems. The enzymatic activity or expression of PAL (phenylalanine ammonia-lyase), CHS (chalcone synthase), CHI (chalcone isomerase), and FLS (flavonol synthase) are integral components of the phenylpropanoid pathway, which leads to the biosynthesis of flavonoids and is observed to be stimulated either directly or indirectly in response to various light conditions (Zhang et al., 2018). Flavonoids have a pivotal role in conferring numerous advantageous attributes to plants, notably their anti-oxidative and anti-inflammatory characteristics. Different plant species need different light regimes to produce the highest levels of certain secondary metabolites and flavonoids (Singh et al., 2023). For example, *Lithocarpus litseifolius* (A. Li et al., 2016) and *Zingiber officinale* (Ghasemzadeh et al., 2010) both produced the most flavonoids when exposed to low light, while *Glycine max* produced more flavonoids when exposed to high light intensity (Yuan et al., 2015). For *Anoectochilus roxburghii*, however, a mix of R and B light is better for growth and the production of secondary metabolites than either R or B light alone (Gam et al., 2020). They also revealed that when plants were exposed to red and blue light, the amount of flavonoids in the plant increased significantly, as did the activity of key genes like PAL, CHS, CHI, and FLS compared to control and other light conditions. In many reports, it has been seen that the anti-oxidant system is associated with the augmentation of secondary metabolites in many plant species (C.-C. Chen et al., 2020; T. D. Silva et al., 2020). Alvarenga et al. (2015) reported that *Achillea millefolium* plants subjected to R and green LEDs elicited higher levels of monoterpenes and sesquiterpenes in an in-vitro environment. In *Plectranthus amboinicus*, the carvacrol content has been enhanced under R light exposure (S. T. Silva et al., 2017), while the carvacrol level increased in *Lippia gracilis* under the application of predominantly B light (Lazzarini et al., 2018). These findings inferred that the effects of light quality vary significantly from species to species. de Hsie et al. (2019) reported that B LED light stimulated limonene and myrcene levels under in-vitro-conditions in *Lippia rotundifolia*; however, a combination of the R and B lights enhanced the content of z-ocimenone. The impact of light extends to both primary and secondary metabolisms. Specifically, light has a direct correlation with carbohydrate production, which is a fundamental aspect of the photosynthetic process (Miyagi et al., 2017). Additionally, light affects secondary metabolism, which includes various molecular and physiological responses. It can influence the gene expression associated with secondary metabolite production as well as the enzymatic activity and biosynthesis of flavonoids, phenolic compounds, anthocyanin, essential oils, monoterpenes, sesquiterpenes, triterpenes, and other compounds (Altonen et al., 2020).

A sesquiterpenoid compound, artemisinin, exclusively obtained from *A. annua* (Family- Asteraceae), has anti-malarial, anti-microbial, and anti-cancerous properties. *A. annua* is employed in traditional medicine as a targeting agent against microbial, inflammatory, oxidant, leishmanial, tumor, and diabetic agents (Donato et al., 2015; Mirbehbahani et al., 2020; Sanja et al., 2012). Despite *A. annua* being known for its medicinal properties, low artemisinin yields are associated with more expensive extraction and purification methods. Therefore, *A. annua* has been the focus of researchers to date.

In our study, we used the Raman spectroscopy technique for the first time to analyze the valuable compounds present in situ after applying different light spectra to *A. annua*. Raman spectroscopy has a significant advantage as an *in-vivo* technique for examining highly complex samples in their environments. It has the capability of simultaneously analyzing multiple molecular species. The Raman spectroscopy technique has been identified as being highly advantageous over chromatographic techniques like HPLC (High-Performance Liquid Chromatography) and GCMS (Gas Chromatography-Mass Spectrometry) for non-invasive analysis of unaltered, intact plant tissue, avoiding sample preparation procedures (Hou et al., 2019). The effect of light quality was investigated in *A. annua* in terms of physiological aspects, defense mechanisms of the plant, and the qualitative and quantitative presence or absence of bioactive compounds like essential oils, flavonoids, and phenolics. In conjunction with these, transcriptomic parameter analysis has also been conducted to determine whether the plant's responses are only short-term metabolic adaptations or related to transcriptional modifications.

2. Methods and materials

2.1. Source of plant material

A. annua seeds were collected from the Botanical Gardens of Banaras Hindu University, Varanasi, and disinfected for 10 min with a solution of sodium hypochlorite (0.1%). The seeds were then cleaned by washing them with double distilled water and sowing them in a germination tray which contained soil and sand in 1:1 proportion. The tray was kept in the dark for a week before being moved to the growth chamber, which was kept at 25°C, 40 μmol. m^{-2}. s^{-1} light intensity, and 16 h/8 h light and dark conditions. Twenty-one days after germination, plantlets were transferred to half-strength Hoagland media (Hoagland and Arnon, 1950). Further, the acclimatized plants were used for experimental purposes.

2.2. Experimental layout and light-quality treatment

The acclimatized 8–10 leaf-stage plants in half-strength Hoagland media were placed under an experimental panel for the treatment of different wavelengths of light. All the plants were exposed to monochromatic, dichromatic, and white LED light conditions for ten days. The following treatments were given to the plants: monochromatic red LED light (R) and blue LED light (B) with 100% maximum intensity at 657 nm and 457 nm, respectively, along with a combination of red and blue light (RB) in a 1:1 ratio with 50% red light and 50% blue light. A multi-wavelength 400–700 nm white LED light (W) source was used as a control. The intensity of light was measured as PPFD from the canopy of the plant and maintained at around 200 μmol. m^{-2}. s^{-1} for each light regime, which was measured using a lux meter and adjusted for the distance of the plant canopy from the light source. The plants were kept at 25 ± 2 °C with a 16/8 h light/dark regime maintained by a timer and a relative humidity of 60%. The culture racks were covered with black cloth to avoid interference with the other light sources, and LEDs were placed at the top. During the light treatment process, a daily rotation and replacement of plant positions were implemented to avoid the positional effect and ensure the accuracy of the experimental outcomes. After 10 days of exposure, the plants were harvested for further experimental purposes. The experimental treatments were conducted with five replicates, and each treatment and assay were carried out three times.

2.3. Total chlorophyll content, carotenoid, and anthocyanin estimation

The chlorophyll pigment extraction and determination from the leaf samples were performed by following the method of Porra et al. (1989). After 10 days of light-quality treatment, 200 mg of fresh leaves were harvested from a single plant, and an assay was carried out with five replicates for both the treated and control plants. Samples were homogenized in 80% acetone, filtered with a muslin cloth, and centrifuged for 15 min at 6000 x g. The supernatant of each sample was measured by a double-beam spectrophotometer (Hitachi U-2910) at wavelengths of 480 nm and 580 nm for the detection of carotenoids and at 663 nm and 645 nm for chlorophylls a and b, respectively. The calculations of the photosynthetic pigments and total carotenoid contents were done as described by Porra et al. (1989). Anthocyanin estimation was done according to Mancinelli et al. (1975). Briefly, 100 mg of fresh leaves (treated and control) were homogenized in acidified methanol (1HCl: 99 methanol). After incubation for 24 h at 0 °C the extracted volume was 10 ml by dilution. Thereafter, the absorbance was measured at a wavelength of 530 nm using a double-beam spectrophotometer (Hitachi U-2910, Tokyo, Japan).

2.4. Chlorophyll fluorescence assessment

PAM-2500 (pulse amplitude modulation) with data acquisition software Pam-Win3 was used to measure chlorophyll fluorescence from the leaf surfaces of control and light-quality treated plants. Before recording data, plants were placed in a dark condition (20 min) for adaptation. To determine the minimum fluorescence (Fo), leaves were exposed to the light of low irradiance, and for maximum fluorescence (Fm) levels, plant samples were exposed to the same surface at an excitation pulse (3000 μmol. m^{-2}. s^{-1}). The other fluorescence parameters were evaluated in both treated (light quality) and control (white light) plant leaves, including photochemical quenching (qP), electron transport rate (ETR), the relative quantum efficiency of PSII photochemistry (ϕPSII), non-photochemical quenching (NPQ), maximum fluorescence (Fm), minimum fluorescence (Fo), variable fluorescence (Fv), and variable fluorescence to the maximum fluorescence ratio (Fv/Fm).

2.5. Estimation of total phenolic and flavonoid content

To determine the total phenolic content of control and treated plant leaves, catechol was used as the reference concentration. 200 mg of fresh leaves were taken from a single plant, and the assay was carried out with five replicates for both the treated and control plants. The leaf sample was heated at 90°C in a 10 ml mixture of 1.2 M HCL and 50% aqueous ethanol solution, as described by Imeh and Khokhar (2002). Following this, 100 μL, 1.58 ml, and 1.9 M of Folin-Ciocalteu reagent, water, and sodium carbonate, respectively, were added to the warm solution. After incubating this mixture at a temperature of 40°C for 30 min, the absorbance was taken at 765 nm. The calculation of the phenolic contents was done by catechol equivalents using the standard curve of eight different catechol concentrations. The flavonoid content was assessed by Chang et al. (2002) an aluminum chloride assay in control and treated plants under different light-quality conditions and quercetin (Q3001) as a calibration reference. The 0.1 g dried leaf sample was crushed in 25 ml of ethanol (95%), then placed on a shaker and rotated at a speed of 200 revolutions per minute for the next 24 h. Additionally, 2 ml of extract was mixed in the reaction mixture containing 0.1 ml, 10%, and 2.8 ml of potassium acetate (1 M), aluminium chloride, and distilled water, respectively. The absorbance was measured at 415 nm after incubation for 30 min at room temperature.

2.6. Histochemical characterization of lignin content

As per the method given by Dhaka et al. (2019), lignin estimation was carried out using 1 g of dry leaf samples from control as well as treated plants and digested with 72% H_2SO_4 at 47°C. After digestion, the samples were autoclaved at 121°C and 1 atm pressure for 30 min. The samples were filtered through to segregate the soluble and insoluble constituents, followed by absorbance at 280 nm and 215 nm for each sample. The concentration of lignin was determined by applying the given formula-:

$$S = (4{\cdot}53A215\text{-}A280)/300{\cdot}$$

Where A280 (O.D. value at 280 nm) = 0.68 F + 18 S and.

A215 (O.D. value at 215 nm) = 0.15 F + 70 S (S = soluble lignin content in g/L, F = concentration of furfural in g/L, the molar absorptive values for furfural at 280 nm is 0.68 and at 215 nm is 0.15).

Similarly, the molar absorptive values of soluble lignin at 280 nm and 215 nm are 18 and 70, respectively. The determination of lignin content was done by taking total lignin (soluble and insoluble) and expressing it in mg/g cell wall.

2.7. In-vivo staining of ROS (reactive oxygen species)

The nitroblue tetrazolium staining (NBT) method was used to determine whether treated and controlled leaves accumulated superoxide radicals (O^{-2}), according to Rao and Davis (1999). The leaves of the plants grown under light conditions and control were transferred to a

solution containing 5 mM NBT and 10 mM phosphate buffer and incubated for 10 h. Subsequently, leaves were bleached with a solution containing 3 ethanol /1 acetic acid/1 glycerol (v/v/v) and heated to a temperature of 100 °C. For the DAB (3,3-diaminobenzidine) staining method we followed according to Thordal-Christensen et al. (1997), the control and different light conditions grown leaves were subjected to immersion in a 6 mM solution of 3,3-diaminobenzidine and incubated under dark conditions for 8 h. Subsequently, the leaves were subjected to the aforementioned bleaching procedure. The photographs were captured using a computer equipped with a Dewinter image microscope.

2.8. Activity of antioxidant enzymes

500 mg of fresh leaves were harvested from a single plant, and the assay was carried out with five replicates for both the treated and control plants and then homogenized using 5 ml of extraction buffer (1 mM phenylmethylsulfonyl fluoride (PFMS), 50 mM phosphate buffer, 2 mM ethylenediaminetetraacetic acid (EDTA), and 1% polyvinylpyrrolidone (PVP)). The resultant supernatant was obtained through centrifugation at 12000 x g for 15 min at 4°C and kept at 4°C for further estimation of antioxidant enzymes. The activity of the SOD (superoxide dismutase) enzyme was determined by Beauchamp and Fridovich (1971). For measuring the activity of the SOD enzyme, a reaction mixture had 13 mM methionine, 50 mM sodium phosphate buffer (pH = 7.8), 75 M NBT, 2 M riboflavin, and 100 nM EDTA along with enzyme extract. The activity of the SOD enzyme was quantified by the NBT inhibition assay of photochemical reduction, and after incubating the reaction mixture in light, absorbance was taken at 560 nm. Further, as described by Aebi (1984), the activity of CAT (catalase) enzymes was measured by carrying out H_2O_2 decomposition using a solution having 50 mM sodium phosphate buffer (pH = 7) and 24 mM H_2O_2. The absorbance of H_2O_2 decomposition was measured at 240 nm. The method of Schaedle and Bassham (1977) was used to estimate GR (glutathione reductase) activity. Enzyme extract, potassium phosphate buffer (50 mM) (pH=7.8), Na_2EDTA (2 mM), NADPH (0.15 mM), and glutathione oxidized (0.5 mM) were used in the reaction mixture for the same. The absorbance for NADPH oxidation (a reaction inhibitor) was measured at 340 nm. For the assessment of POD (peroxidase) activity, 0.1 g of the leaf was homogenized in a cold sodium-phosphate buffer of 100 mM (pH = 7), and 5 mM cysteine, then centrifuged at 10000 x g for 15 min 2 ml of 125 mM phosphate buffer at (pH = 7), 50 M H_2O_2, 50 M pyrogallol, and 1 ml of enzyme extract were added to the reaction solution. The solution was left at 25°C for 5 min, and absorbance was taken at 430 nm Britton and Mehley (1955).

2.9. Identification of artemisinin content through HPLC

Extraction and quantification of artemisinin from the leaves of *A. annua* were performed via HPLC according to S.-S. Zhao and Zeng (1985) with minute modifications. 100 mg of dry leaf (at room temperature for 1 week) were collected from a single plant, and the process was carried out with five replicates for both the treated and control plants homogenized with 20 ml of petroleum ether for 3 h in a soxhlet extractor. After ultrasonication and filtration under vacuum, the samples were desiccated by evaporation, and subsequently, the filtrate was added to 1 ml of ethanol. Thereafter, 100 ml of the supernatant was collected after centrifugation for 1 min at 10,000 g and mixed in 0.4 ml of a 0.2% (w/v) solution of NaOH for 35 min at 45°C temperature. Before HPLC analysis, the solution was left at normal temperature for cooling and then treated with 0.5 ml of acetic acid (0.05 M) and filtered with a Millipore filter with a size of 0.45 μm. The sample was eluted with 2:3 v/v methanol and sodium phosphate buffer solutions using an HPLC system equipped with a water 600E condition and a 150 × 4.6 mm Hypersil BDS C8 column at a flow rate of 1 ml/min, and the peaks were observed at 260 nm. The calibration curve and results of standard artemisinin from Sigma Aldrich were matched to determine the concentration of the samples.

2.10. Morphological examination of leaf surface with SEM (scanning electron microscope)

To analyze the surface structures (trichomes and stomata) of leaves from light-quality-treated and control plants (fully expanded third leaf) under light-quality exposure, scanning electron microscopy was used. Sample preparation was carried out according to Hess (1966). Leaves were first fixed in sodium phosphate buffer (pH = 7.2) using 2.5% glutaraldehyde and then transferred into an ethanolic dehydration series and left to dry for 30 min. The fully dried pieces of leaves were coated with a thin layer of gold and observed via scanning electron microscopy (Carl Zeiss, EVO-18, Germany).

2.11. In situ assessment of leaf via Raman spectroscopy

A confocal Raman imaging microscope (WITec alpha300) was used for the characterization and surface analysis of control and treated *A. annua* leaves. Since it is capable of detecting signals from a distance of 10 cm, it is regarded as a remote sensing system. This method was conducted using a continuous-wave laser source with a wavelength of 532 nm and a leaf spot size of 200 μm. Control and light-quality exposed leaves were directly placed on the specimen holder without being physically separated from the tested plant. Thus, the imaging approach is non-destructive, and the sample does not need to be fixed or stained. The use of CCD (charged-coupled device) cameras assisted in the detection of scattered radiation induced by the lasers, which had air-based cooling systems. The laser signals fell on plant tissue that was adjusted so that live cells were not affected (for spectroscopy analysis, it was 10 mW with a 10 s acquisition time). Raman spectra are dominated by intrinsic fluorescence emitted from the molecules present in the plant tissues, as per the methodology of Altangerel et al. (2017) with minor modifications.

2.12. RNA Isolation and Transcript Analysis

Control and light-quality-treated fresh leaf tissues were taken for the isolation of RNA using the TRIZOL reagent (GIBCOBRL) as per the protocol of the manufacturer. Isolated RNA was measured by a Nano-Drop spectrophotometer (Thermo Scientific). Software Primers 3 was used to design the primers for artemisinin and flavonoid biosynthetic pathway-regulated genes for transcript analysis (Table S1). Using a thermal cycler (Bio-Rad), semi-quantitative RT-PCR was carried out to investigate the expression profile of genes. RT-PCR product intensities were observed on a 2% agarose gel with the GelDOC EZ imager (Bio-Rad) and Quantity One software (Bio-Rad). The endogenous gene expression of *ACTIN* was used to normalize the transcript value of targeted genes. The relative CT (threshold cycle) approach was used to determine the qRT-PCR amplification values (Pandey, Meena, Rai, and Pandey-Rai, 2016). Melting curves were utilized to determine primer amplification fidelity and normalized fold changes were calculated for each gene expression.

2.13. Statistical analysis

The given experiments were repeated three times, with a minimum of five biological replicates per treatment and control. The data were depicted as mean value and ± standard error. SPSS Inc. version 16.0 was used for one-way ANOVA statistical analysis, and Duncan's multiple test range ($P < 0.05$) was employed for the statistical significance determination. Graph-pad prism (version 5.01) was used to create the graphic depiction. The Past3 software was used for the visualization of the correlation study. Average linking and the Euclidean distance matrix were used to create the heat map with the help of Bioconductor-R (http://www.bioconductor.org).

3. Results

3.1. Light-quality treatments cause morphological alterations

The morphological indexes of *A. annua*, including total plant height, petiole length, leaf area, fresh weight, dry weight, and shoot length, are directly influenced by the light quality (Table 1 and Fig. S1). The plantlets exhibited the highest level of plant height when subjected to red light (R), resulting in a 10.2% increase compared to W light. This observation suggests that R light has a beneficial effect on plant height. In contrast, the exposure to B light resulted in a reduction of plant height by up to 15.9%, while the RB light exposure did not exhibit any significant change as compared to W light. A similar outcome was also noted in relation to the shoot length. In contrast to W light, the findings revealed that the highest leaf area and longest petiole were found during B light exposure; however, no significant disparities were observed between R and W light exposures. A significant increase of 130.5% in leaf area was recorded under B light conditions, while an 81.2% increase was observed during RB light exposure as compared to W light. The maximum fresh weight and dry weight were recorded under B light at 16.2% and 31%, respectively. In contrast, under R light, there was a reduction of 18.8% and 31% in fresh weight and dry weight, respectively, compared to W light. The aforementioned findings revealed that the plantlets had distinct and diverse effects on the different light regimes.

3.2. Predominantly B light is responsible for promoting photosynthetic pigment accumulation

The result of the chlorophyll and carotenoid levels in the leaves of *A. annua* is pertaining in Fig. 3. There was a significant variation in the total pigment content among the treatments in comparison to the plants growing under W light conditions. In this study, it was shown that exposure to B light resulted in the highest levels of Chlorophyll a, Chlorophyll b, and total chlorophyll content in the leaves of *A. annua* followed by RB and W light exposures. The R light had the lowest content. In contrast to the W light, B light resulted in increments of 88.2%, 60.2%, and 162% for total chlorophyll, chlorophyll a, and chlorophyll b content, respectively. In addition, the presence of RB light also resulted in a significant increment of 18.6% and 3.9% for chlorophyll a and total chlorophyll respectively. No significant variation was found in carotenoid content across the treatments and control, except R light. In contrast to the W light, the total anthocyanin content in *A. annua* plantlets was found to be significantly higher in all treatments. The B light exhibited the greatest increment of anthocyanin content, demonstrating 107.9%, while the RB light displayed a 62% rise as compared to the W light. Nevertheless, it is worth noting that under R light exposure, there is a modest increase of 32.7%, as depicted in Fig. 4. The findings suggest that the quality of light has the potential effect on photosynthesis by influencing the functionality of photosynthetic pigments.

3.3. Impact of light quality exposure on chlorophyll fluorescence parameters

After 10 days of exposure to various light spectrums, chlorophyll fluorescence parameters were examined in *A. annua* plantlets, as indicated in Table 1. It was reported that the maximum quantum efficiency (Fv/Fm) was appreciably greater in B light-grown leaves. As per our observations, the Fv/Fm increased by 4% in B light and decreased by 8.8% under R light exposure compared to W light; however, no significant change was observed under RB light conditions. The photochemical quenching (qP) and relative quantum efficiency of PSII (ϕPSII) exhibited higher values under B and RB light conditions, with increments of 81.7%, 70.8%, and 3%, 38.2%, respectively, in contrast with W light. Conversely, red (R) light resulted in reductions of 73.3% and 33.5% compared to W light. Moreover, plants grown under R light demonstrated a higher non-photochemical quenching (NPQ) compared to W light conditions, with an increment of 22.7%, and declined under RB (13.3%) and B (41.4%) light conditions. Additionally, ETR was significantly influenced by B light, followed by RB light, with increments of 192% and 109.7%, respectively, and a reduction of 38% under R light as compared to W light.

3.4. Dichromatic light enhances the total flavonoids, phenols, and lignin content

Our results showed that the accumulation of flavonoid biosynthesis in *A. annua* is not only influenced by single light wavelengths but also by the combination or relative proportions of light conditions. Among all the light treatments, the RB light caused the highest production of total flavonoid in contrast to single-wavelength light, showing an increase of 4.7-fold in total flavonoid content in comparison to W light (Fig. 5A). Single-wavelength exposure of B and R light also increased the total flavonoid contents by 3.3 and 2-fold, respectively, in contrast to W light. However, in our experiment, the total phenolic content was observed to be markedly enhanced under exposure to B light and RB light, followed by R light, as shown in Fig. 5B. The single-wavelength B light immensely increased the phenolic content by 160.2%, followed by RB light (139.5%) in contrast to W light. Moreover, the accumulation of phenols under the R light was 37.4% higher than under the W light. There was also a significant difference in the lignin deposition observed between the light-quality treatments and the control plant. It was found that the RB light showed enhancement by 44%, followed by the B light (37%), and the R light (20%) in contrast to the W light (Fig. 5C). These results suggest that the use of colored light (differential wavelength) and their combinations as elicitors are promising approaches for enhancing the alteration of cell wall components and lignin deposition.

Table 1
Alterations in morphological characteristics and chlorophyll fluorescence parameters of *Artemisia annua* in response to different light quality exposure, white (W), red (R), blue (B), and red-blue (RB) light.

Parameters	White light	Red light	Blue light	Red + Blue Light
Plant fresh weight (g)	1.33 ± 0.15^{b}	1.08 ± 0.16^{c}	1.56 ± 0.13^{a}	1.35 ± 0.13^{b}
Plant height (cm)	31.26 ± 0.55^{ab}	34.46 ± 0.59^{a}	26.26 ± 0.67^{b}	31.16 ± 1.08^{ab}
Leaf area (cm^2)	6.81 ± 0.78^{b}	6.93 ± 0.67^{b}	15.71 ± 0.76^{a}	12.353 ± 0.44^{ab}
Petiole length (cm)	1.5 ± 0.14^{b}	1.43 ± 0.26^{b}	2.7 ± 0.38^{a}	2.13 ± 0.91^{b}
Fv/Fm	0.77 ± 0.07^{ab}	0.70 ± 0.04^{c}	0.80 ± 0.04^{a}	0.78 ± 0.05^{b}
ϕPSII	0.12 ± 0.08^{bc}	0.08 ± 0.07^{c}	0.22 ± 0.10^{a}	0.17 ± 0.09^{ab}
qP	0.10 ± 0.09^{b}	0.02 ± 0.03^{c}	0.19 ± 0.12^{a}	0.10 ± 0.08^{b}
NPQ	0.53 ± 0.10^{ab}	0.65 ± 0.13^{a}	0.31 ± 0.1^{c}	0.46 ± 0.15^{b}
ETR	4.63 ± 0.39^{c}	2.86 ± 0.36^{d}	13.53 ± 0.54^{a}	9.72 ± 0.45^{b}

Values represent the average ± standard error of five separate replicates. In the column, letters indicate the significant variations according to Duncan's multiple range test ($P < 0.05$). One-way ANOVA was applied for data analysis.

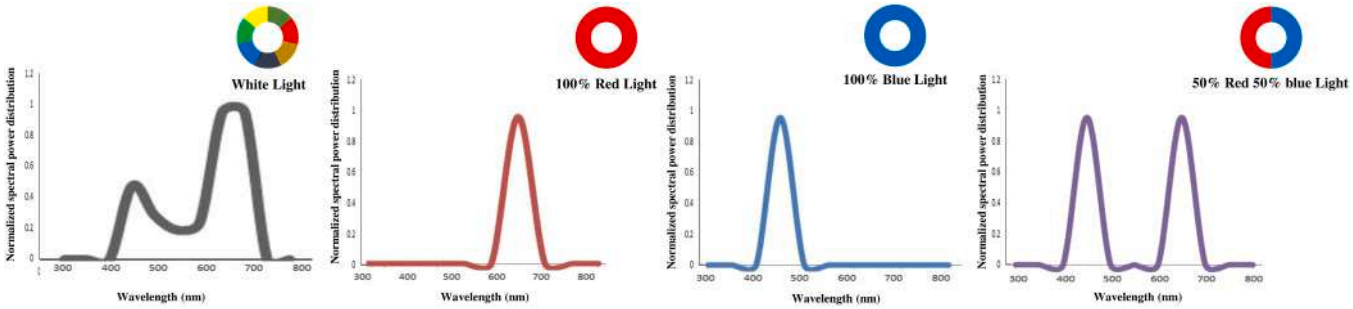

Fig. 1. The irradiance of different LED light spectra white (W), red (R), blue (B), and red-blue (RB) light on *Artemisia annua* plantlets.

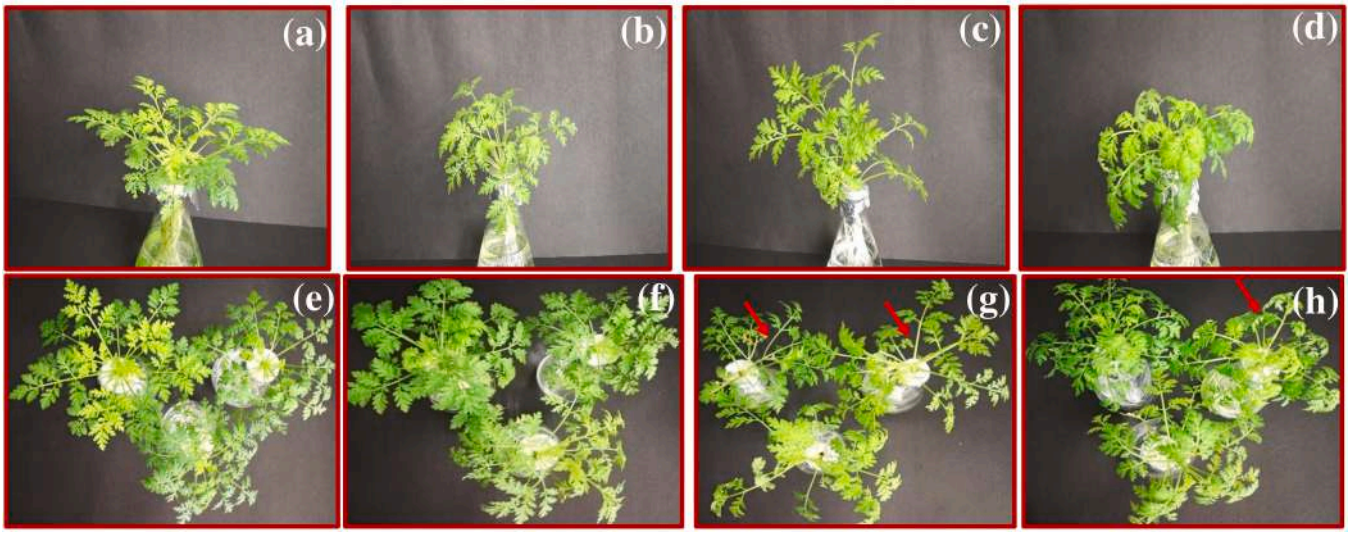

Fig. 2. Exposure to various light spectra and their effect on plant growth and morphology in *Artemisia annua*; (a, e) white light, (b, f) red light, (c, g) blue light, and (d, h) RB light. Examine the morphological differences in plantlets of *Artemisia annua* and the variation in petiole elongation and leaf morphology (indicated by a red arrow) under blue and RB light.

3.5. The combination of R and B light stimulates ROS accumulation and the activity of antioxidant enzymes

The assessment of the classic stress markers, superoxide radical (O^{-2}) and H_2O_2 was performed to measure oxidative imbalance and damage under different light conditions (Fig. 6). RB light exposure exhibited the highest H_2O_2, accumulation, followed by B light and R light, in a contest with W light-grown plants. The DAB (3,3-diaminobenzidine) staining produces a reddish-brown color at the site of H_2O_2 accumulation, whose intensity can be positively correlated with the level of H_2O_2 accumulation. The level of O^{-2} generation was marked by the extent of the blue-colored formazone formation in the leaves. The accumulation pattern of O^{-2} follows the same pattern as that of H_2O_2 accumulation in the leaves (Fig. 6).

The antioxidant defense system in *A. annua* plants was activated in response to different light conditions, as shown by the activity of SOD, POD, GR, and CAT in this study (Fig. 7). Among the different treatments, RB and B light exposure increased SOD, POD, and CAT activities the most. This was followed by R light exposure, as compared to the effects of W light. Whereas, in contrast to W light, no significant alteration in GR activity has been detected under exposure to R light. The application of RB, B, and R treatments resulted in a respective increase of 3.32, 2.03, and 1.9-fold, respectively, for SOD activity compared to the W light. The exposure to R light did not elicit any significant alteration in GR activity; however, the exposure to RB and B lights resulted in a respective increase of 4.8 and 2-fold in GR activity. The study showed that the activity of CAT was significantly elevated, exhibiting 8, 4.5, and 2.6-fold increases under RB, B, and R light exposures as compared with W light. Additionally, in contrast with the W light condition, the RB, B, and R light exposures exhibited a notable increase in POD activity, with a fold increase of 2.9, 2, and 1.4-fold, respectively.

3.6. Light quality influences surface structure in A. annua

SEM examination of the glandular trichrome, the location of artemisinin biosynthesis and storage in *A. annua* under various LED light treatments alone or in combination. The micrographs of SEM revealed that the surface exposed to RB and B lights showed more stomatal density and a larger size of stomata in contrast to W light. The structure of the glandular trichomes indicated that their size, specifically in terms of width, exhibited an increase under RB and B light treatments as compared to the size of glandular trichomes in W light conditions. The details can be visualized in Fig. 8.

3.7. In-vivo detection of leaf compounds via Raman spectroscopy under varying light conditions

In this study, we used the Raman spectroscopy technique, which is a powerful, fast, and non-invasive method for in situ assessment of metabolites and quality analysis (Lalani, Kitutu, Clarke, and Kaur, 2017). It is customary in the analysis of Raman scattering to evaluate the experimentally measured scattering intensities (absolute intensities) of vibrational modes (Supplementary Fig. 2). In our study, the Raman spectra of the leaves were recorded over ten days on grown plants under

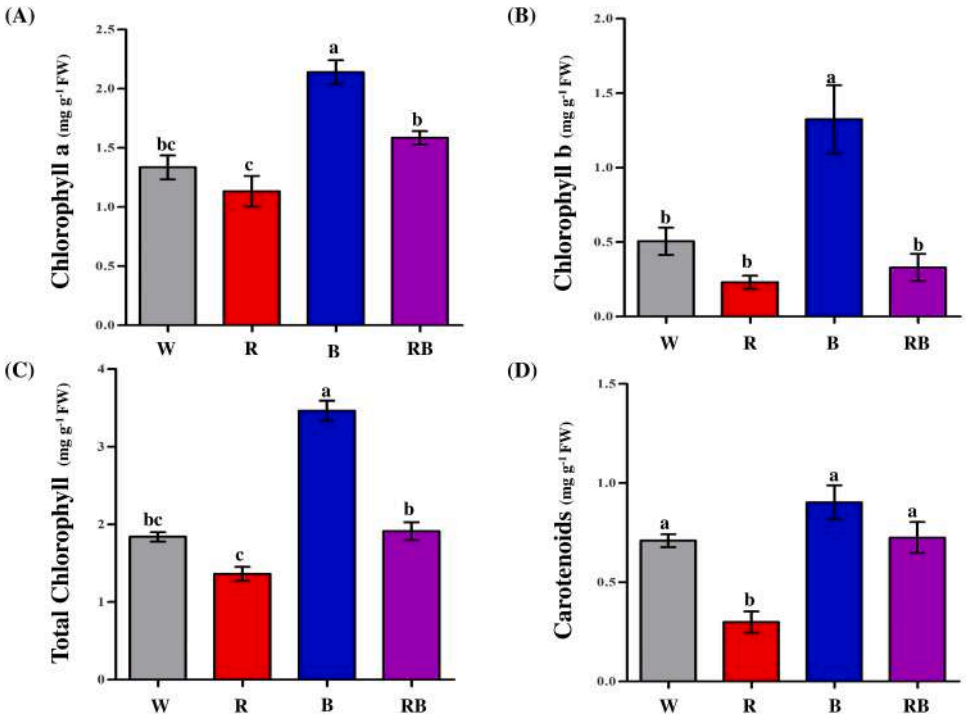

Fig. 3. The impact of different light conditions on the photosynthetic pigments in *Artemisia annua*. The presented data indicated that the mean value with a standard error (± SE) from the three independent studies (n = 3) with distinct letters is significantly different ($P < 0.05$). One-way ANOVA was applied for data analysis.

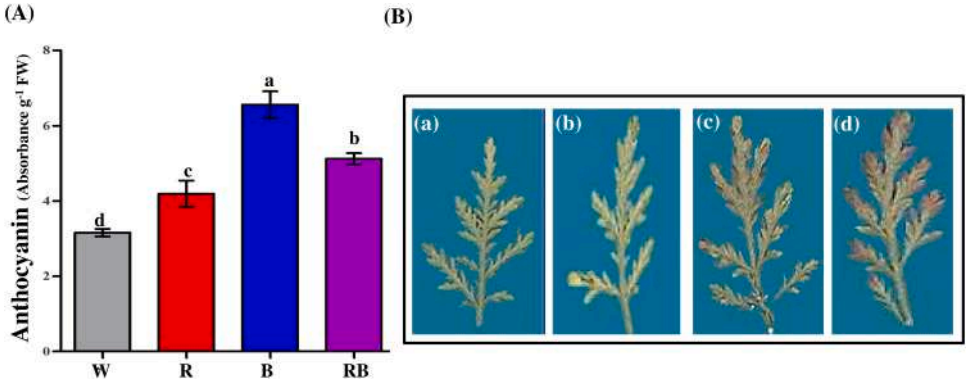

Fig. 4. The impact of various light conditions on anthocyanin accumulation levels in *Artemisia annua*. (A) The vertical bars depict the mean value with a standard error (± SE) obtained from the three independent studies (n = 3) with distinct letters that are significantly different ($P < 0.05$). One-way ANOVA was applied for data analysis. (B) accumulation of anthocyanin content on the leaf surface under light exposure; (a) white light, (b) red light, (c) blue light, and (d) RB light.

different light conditions (R, B, and RB light) and the spectra of the control plants (W light) as well. There were a lot of compounds detected within the range of 200–1800 cm^{-1}, but for this study, we selected only twenty-seven compounds having medicinal potential that can be grouped into terpenes, phenols, flavonoids, and other compounds as given in Table 2. The identified compounds have high medicinal value and antioxidant activity; they are extensively used in the pharmaceutical, food, and nutraceutical industries for the development of novel products. The analyzed compounds exhibited the presence of twelve terpenes, eight phenolic compounds, and seven other compounds. The major peaks were detected at approximately 1526, 1160, and 1007 cm^{-1} in both the treated and control leaves. The spectral peak for carotenoids has been assigned a wavenumber of 1007, 1157, and 1520 cm^{-1} in the literature (Schulz et al., 2007; Baranska et al., 2005a, 2005b). However, our finding has detected shifts in peaks at slightly different wavenumbers under exposure to different lights. Specifically, in the W light condition, peaks were detected at 1009, 1163, and 1526 cm^{-1}. In the presence of R light, peaks were detected at 1007, 1159, and 1525 cm^{-1}, while in the presence of B light, peaks were detected at 1007, 1160, and 1525 cm^{-1}, whereas under the RB condition, peaks were detected at 1526, 1160, and 1007 cm^{-1}. These findings suggest that there is a shift in Raman spectra (Gamsjaeger et al., 2011). The current finding demonstrated that leaves treated with RB light had the highest number of compounds detected, followed by leaves treated with W, B, and R light (Fig. 9). The metabolites kaempferol, quercetin hydrate, epicatechin, chlorogenic acid, caffeic acid, and pectin are mostly found in RB light, kaempferol, quercetin hydrate, epicatechin, chlorogenic acid, and pectin in B light, and caffeic acid in R light. This shows that these metabolites build up in the leaves of *A. annua* plants in a way that depends on the specific light regime. The tabulation of peak intensities for the twenty-seven selected compounds was carried out across the wave number range of 200–1800 cm^{-1}. A comprehensive inventory of the structures and Raman spectra of all selected compounds is summarized in Supplementary Table 1.

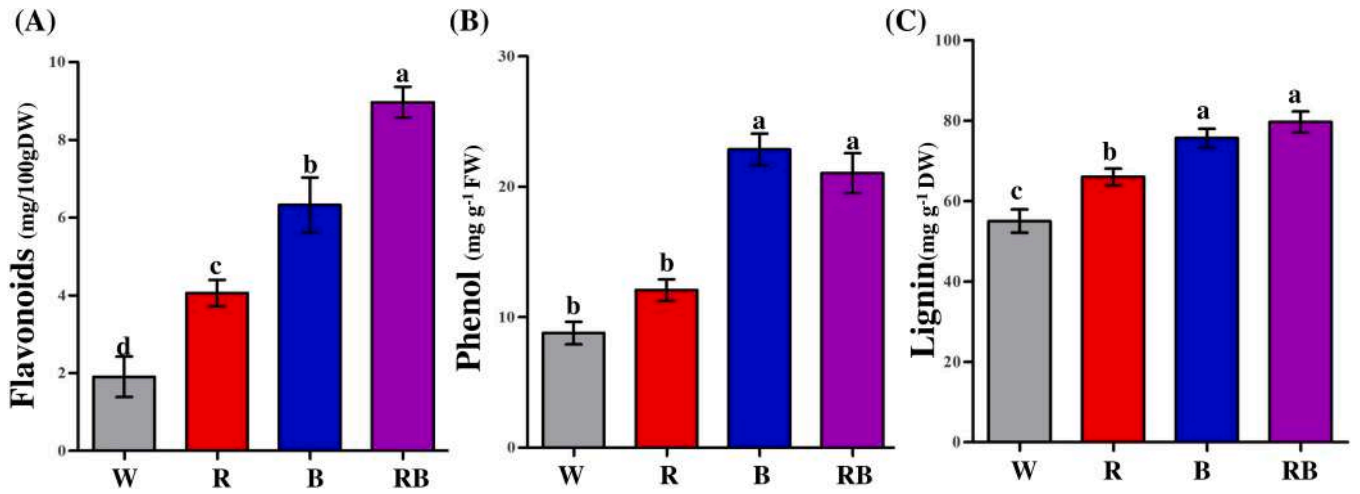

Fig. 5. The impact of light quality on the augmentation of total phenolics, flavonoids, and lignin content in *Artemisia annua*. The graphical bar indicates the mean value with a standard error (± SE) taken from the three independent studies (n = 3) with distinct letters that are significantly different ($P < 0.05$). One-way ANOVA was applied for data analysis.

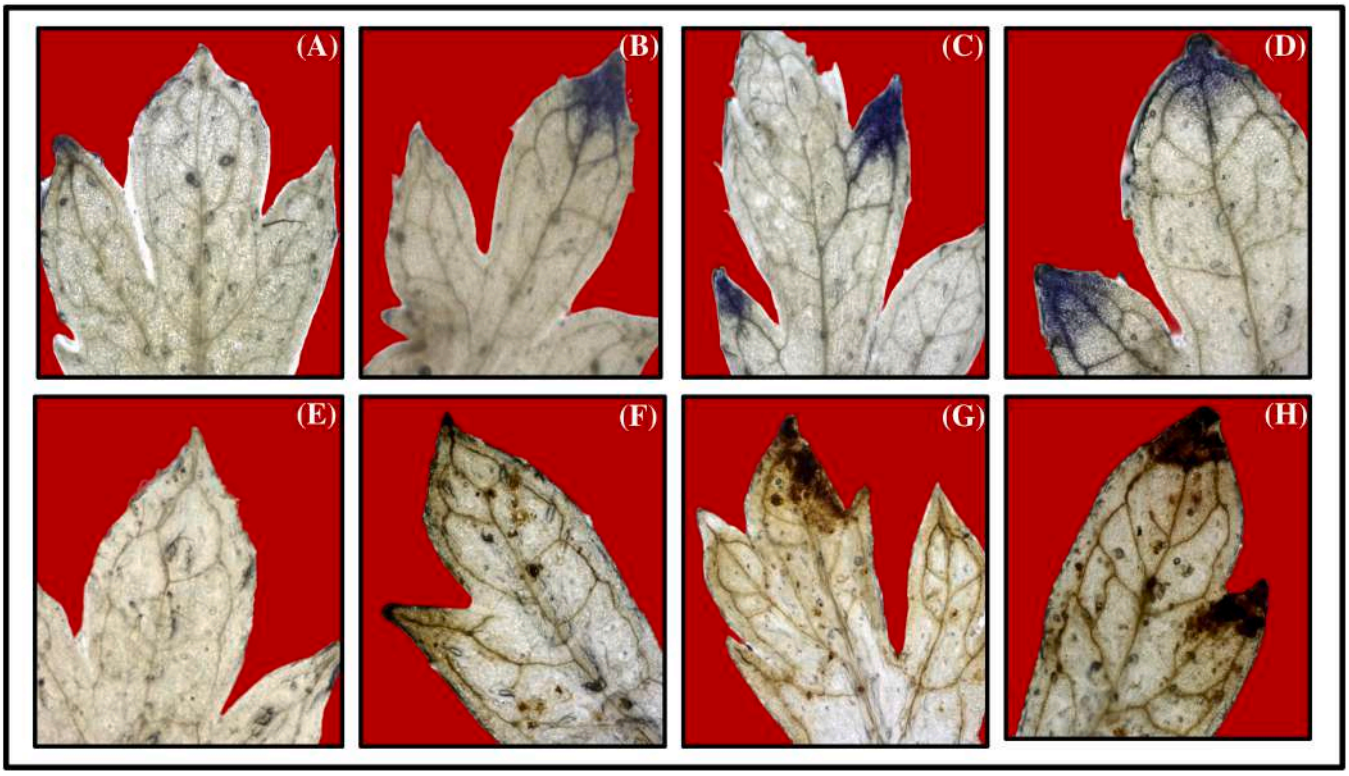

Fig. 6. Superoxide radical and H_2O_2 visualization through NBT (A-D) and DAB (E-H) staining in leaves of *Artemisia annua,* respectively; (A, E) white light, (B, F) red light, (C, G) blue light, and (D, H) RB light.

3.8. Equal R and B light ratio improve artemisinin levels

Artemisinin content was quantified from the dry leaf tissue of *A. annua* by using HPLC. In the HPLC chromatogram, peaks were observed for artemisinin at a retention time of 2 min (Supplementary Fig. 3). The concentration of artemisinin under light treatments was measured with the help of the standard peak area of artemisinin. According to the given graph (Fig. 11), the amount of artemisinin increased the most when exposed to R and B light, by 53.4%, then B light (36.6%), and R light (14.4%) when compared to W light. HPLC chromatogram peak images are given in Fig. S3.

3.9. Expression analysis of secondary metabolite biosynthesis pathway genes under differential light conditions

A total of eight key regulatory genes; *HMGR (3-Hydroxyl-3-methyglutaryl CoA reductase), DXR (1-Deoxy-D-xylulose-5-phosphate Reductoisomerase), DXS (1-Deoxy-D-xylulose-5-phosphate synthase), FPS (Fernasyl diphosphate synthase), ADS (Amorpha-4,11-diene synthase), CYP71AVI (Cytochrome P450 dependent monooxygenase/hydroxylase), DBR2 (Double bond reductase2),* and *ALDH1 (Aldehyde dehydrogenase)* participating in the artemisinin biosynthetic pathway were observed through RT-PCR analysis under LED light (W, R, B, and RB) treatment.

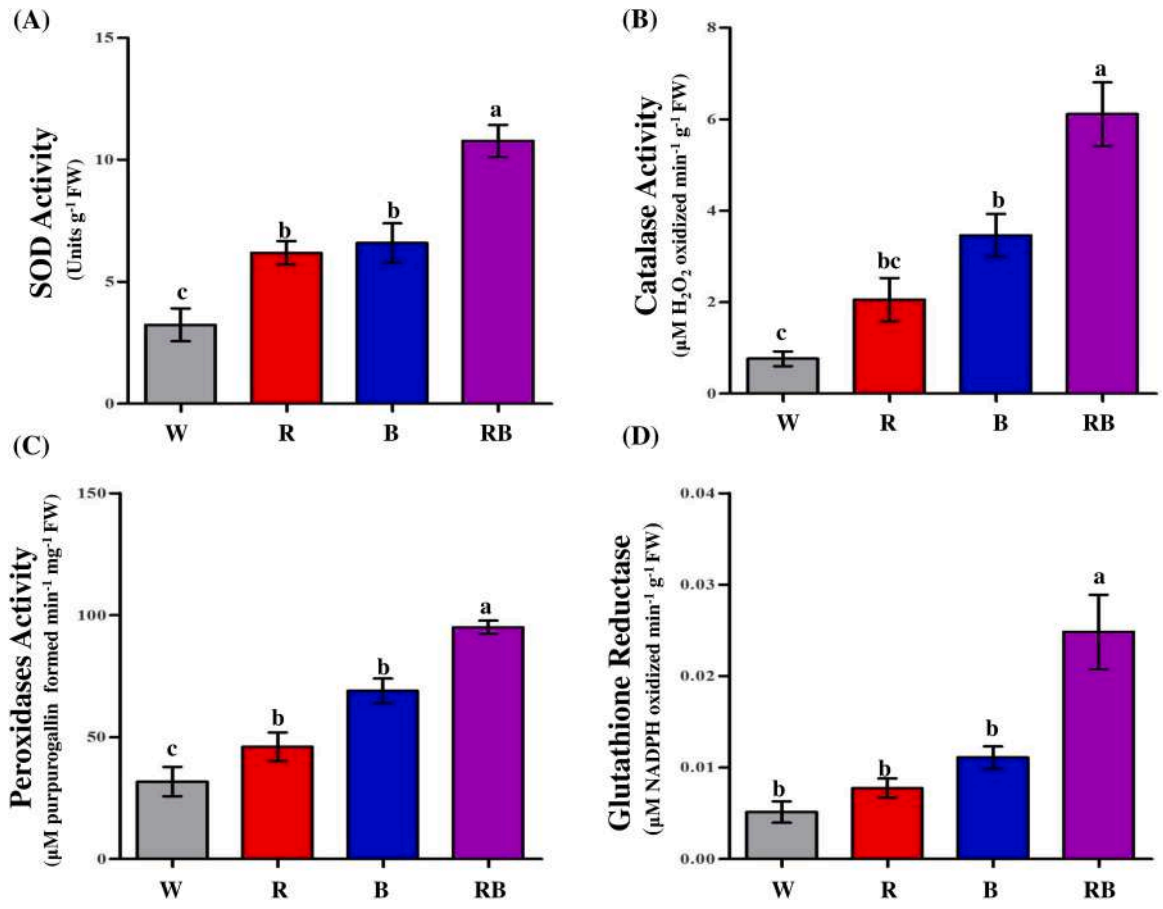

Fig. 7. Light quality effect investigation explores the antioxidant enzyme activity in *Artemisia annua;* (A) activity of superoxide dismutase (SOD); (B) catalase (CAT) activity; (C) peroxidase activity; and (D) glutathione reductase (GR). The vertical bar depicts the mean value with a standard error (± SE) from the three independent studies (n = 3) with distinct letters that are significantly different ($P < 0.05$). One-way ANOVA was applied for data analysis.

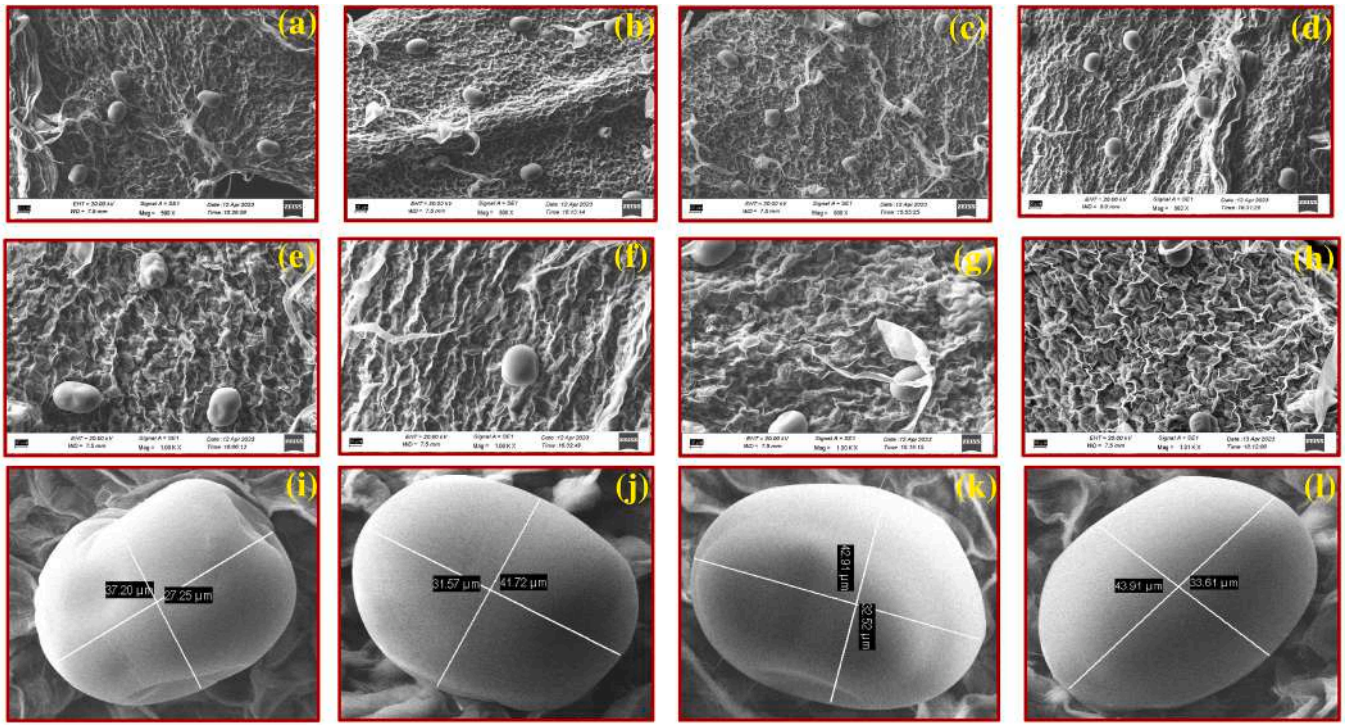

Fig. 8. Scanning electron micrographs show the trichome size (i-l) and stomatal density (e-h) on the leaf surface of *Artemisia annua* under the effects of light conditions: white light (a, e, i), red light (b, f, j), blue light (c, g, k), and a combination of red and blue light (d, h, l).

Table 2
In the Raman spectroscopy study, certain vibrational bands are associated with distinct characteristics of compounds observed under white light, red light, blue light, and a combination of red and blue light exposure in *Artemisia annua*.

Compounds	Wavenumber (cm^{-1}) (Taken from the respective reference)	Wavenumber (cm^{-1}) (White Light)	Peak height [CCD cts]	Wavenumber (cm^{-1}) (Red Light)	Peak height [CCD cts]	Wavenumber (cm^{-1}) (Blue Light)	Peak height [CCD cts]	Wavenumber (cm^{-1}) Red+Blue Light (1:1)	Peak height [CCD cts]
d-Camphor	1741, 651, 1448	1743.14	1.8705	1749.14	2.05805	1752.95	1.0432	1749.85	2.33283
		1444.36	1.46555	662.101	1.13448	1446.21	2.10069	1452.17	3.81513
		659.226	1.57351			657.116	1.29486	667.263	2.58988
p-cymene	1613, 804, 1208	1613.4	1.13778	1217.3	2.70138	1613.33	1.41219	1608.94	4.18117
		1201.03	1.18027			1213.36	1.58681	1215.25	3.8479
		807.425	0.91691			800.578	1.46904		
Limonene	1678, 1645,	1674.77	1.13845	1673.64	1.82388	1677.73	2.82157	1672.96	2.17017
		1642.77	1.06654	1645.35	1.10096			1648.55	4.86556
Terpene-4-ol	1679, 730	1674.77	1.13845	1673.64	1.82388	1677.73	2.82157	1672.96	2.17017
		735.926	1.64875	732.363	1.75402			727.983	2.98008
α terpinene	1611, 1701, 1426, 756	1611.14	1.22535	1433.14	1.33965	1613.33	1.41219	1608.94	4.18117
		1432.05	1.2467					1695.72	1.1965
		759.028	1.23277					1425.3	1.24389
								748.276	5.45056
α pinene	1659, 666	1662.34	0	1645.35	1.10096	1659.86	2.01514	1664.49	2.15347
		659.226	1.57351	662.101	1.13448	657.116	1.29486	667.263	2.58988
β pinene	1643, 645	1642.77	1.06654	1645.35	1.10096	642.569	1.44944	1648.55	4.86556
								643.233	1.55205
1,8 cineole	652	659.226	1.57351	662.101	1.13448	657.116	1.29486	643.233	1.55205
Sabinene	1655, 652	1655.92	1.19126	1645.35	1.10096	1659.86	2.01514	1648.55	4.86556
γ terpene	756, 1701	759.028	1.23277			740.332	1.0475	1695.72	1.1965
β carryophyllene	1632, 1671, 1446	1636.28	1.03631	1673.64	1.82388	1631.02	1.17181	1630.88	3.9174
		1674.77	1.13845	1450.46	1.82047	1677.73	2.82157	1672.96	2.17017
		1444.36	1.46555			1446.21	2.10069	1452.17	3.81513
Artemisinin	724, 1734	724.816	0.170762	732.363	1.75402	740.332	1.0475	727.983	2.98008
		1734.58	2.24564	1733.08	2.16101	1721.35	1.76669	1738.33	2.74083
Kaempferol	1604,1185,1661	1599.18	2.68584	-		1604.27	1.33305	1608.94	4.18117
		1183.43	1.37919		-	1190.95	4.27511	1192.92	9.6809
		1662.34	0			1659.86	2.01514	1664.49	2.15347
Luteolin	1223, 1585, 1589	1227.44	1.68054	1217.3	2.70138	1587.53	2.35938	1234.64	4.42627
		1584.11	1.66953					1592.87	6.05178
Quercetin hydrate	1606, 1590	1611.14	1.22535	-	-	1604.27	1.33305	1608.94	4.18117
		1592.64	0.398553			1587.53	2.35938	1592.87	6.05178
Rutin	1610, 1576	1611.14	1.22535	1573.8	1.56822	1613.33	1.41219	1608.94	4.18117
		1572.86	0.741987			1587.53	2.35938	1567.92	1.70957
Catechin	1633	1629.15	1.48179	1645.35	1.10096	1631.02	1.17181	1630.88	3.9174
Epicatechin	1617	1613.4	1.13778	-	-	1613.33	1.41219	1608.94	4.18117
Chlorogenic acid	1612,1613, 1629	1613.4	1.13778	-	-	1613.33	1.41219	1608.94	4.18117
		1629.15	1.48179			1631.02	1.17181	1630.88	3.9174
Caffeic acid	1614, 1640, 1641	1642.77	1.06654	1645.35	1.10096	-	-	1648.55	4.86556
Carotenoid	1004,1158, 1525	1009.63	2.48777	1007.14	2.58885	1007.46	7.68309	1009.12	14.677
		1163.78	2.47262	1159.76	14.0304	1160.28	28.2716	1158.13	60.2872
		1524.37	6.35409	1525.66	17.7434	1525.36	23.6966	1526.38	56.2487
Anthocyanin	623, 539, 733	628.24	1.80864	624.188	1.06247	542.662	1.5119	620.372	1.54267
		544.439	0.962858	542.207	1.55074	740.332	1.0475	541.587	6.59323
		735.926	1.64875	732.363	1.75402			727.983	2.98008
lignin	1660, 1600, 1604	1605.76	1.46649	-	-	1659.86	2.01514	1664.49	2.15347
								1608.94	4.18117
Phenylanin	1003,	1009.63	2.48777	1007.14	2.58885	1007.46	7.68309	1009.12	14.677
Pectin	747	-	-	-	-	740.332	1.0475	748.276	5.45056
Chlorophyll b	1660		-	-	-	1659.86	2.01514	1664.49	2.15347
Nitrate	1046	1044.09	0.649979	-	-	1061.25	1.24024	1058.71	3.67859

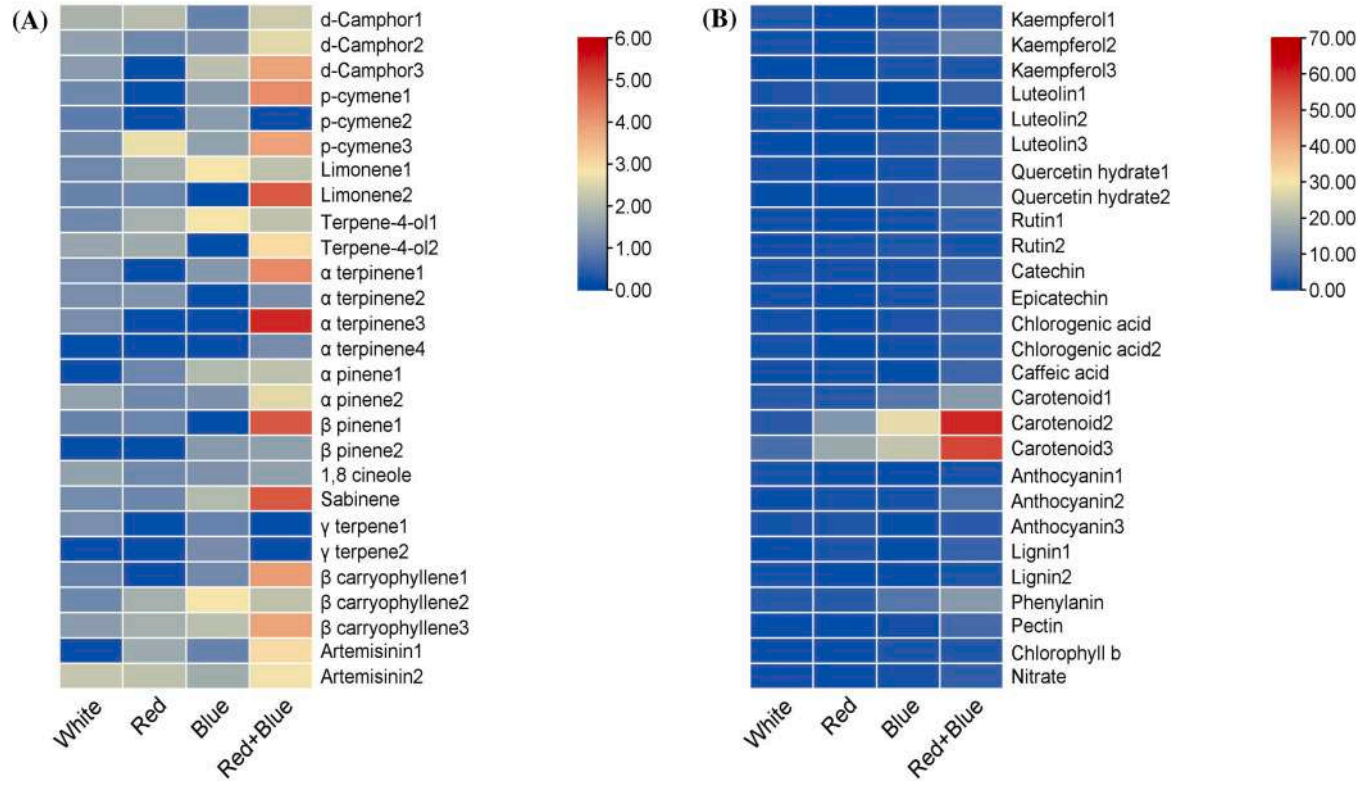

Fig. 9. A heatmap was made that shows the different plant compounds found in *Artemisia annua* that were studied by Raman spectroscopy in different light conditions. (A) represents the terpene compounds. (B) denotes the compounds related to the group of phenolics, flavonoids, and others.

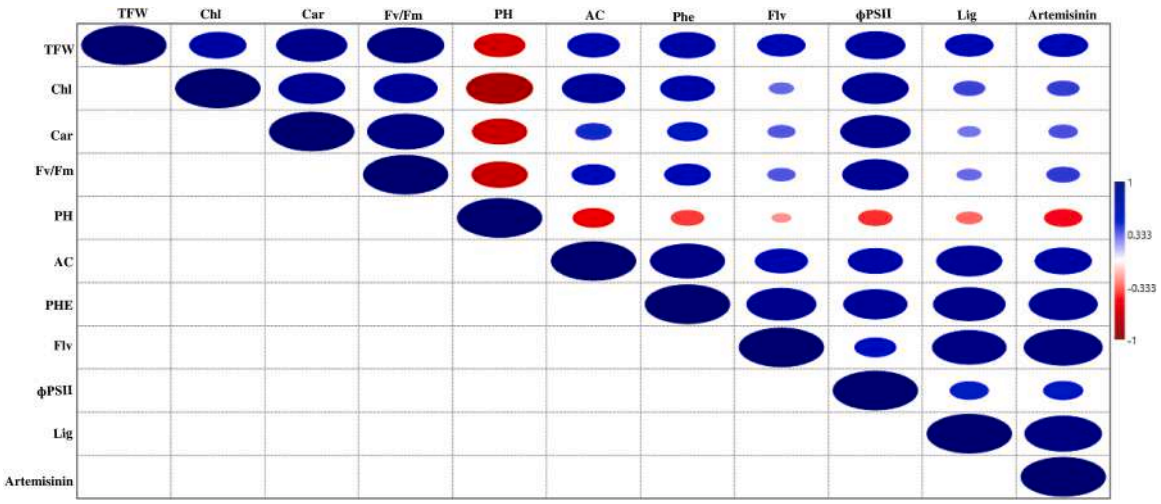

Fig. 10. A symbolic depiction of correlation coefficient analysis between various morphological, physiological, and biochemical traits of *Artemisia annua* under control and different light spectrum effects.

After exposure to different LED lights, the transcript levels of all the genes significantly increased (Fig. 12) concerning W light. The precursors for C5 (IPP/ DMAPP) are facilitated by two distinct processes: the cytosolic MVA (mevalonic acid) pathway and the plastid-based MEP (methylerythritol phosphate) pathway. Compared to control plants, increased C5 building blocks for sesquiterpenoids biosynthesis are possible due to the upregulation of the *HMGR* gene of the MVA pathway, and our results showed fold changes of 3.5, 2.7, and 2 under RB, B, and R lights, respectively. The DXR gene of the MEP pathway exhibited a 3.5-fold increment with RB light exposure, a 3-fold increment under B light exposure, and a 1.8-fold rise with R light exposure in comparison to W light. A similar pattern of expression for the DXS gene was also seen to be upregulated by 2.2-fold, 1.8-fold, and 1.3-fold after treatment with RB, B, and R light, respectively, compared to W light. Among all the genes, *CYP71AVI* was highly up-regulated under RB, B, and R light treatment in 2.2, 2, and 1-fold increments, respectively, as compared to W light. Similar to the *CYP71AV1* gene expression pattern, other genes (*DXS, ADS, DXR, ALDH1, HMGR, DBR2,* and *FPS)* also showed the highest upregulation under the RB light condition, followed by the B, R, and W light conditions. The expression patterns of FPS, ADS, DBR2, and ALDH1 genes clearly showed 3–2.7–1.7, 1.6–1.3–1, 3.3–2.8–1.4, and 4–3.4–1-fold increments when subjected to RB, B, and R light exposure,

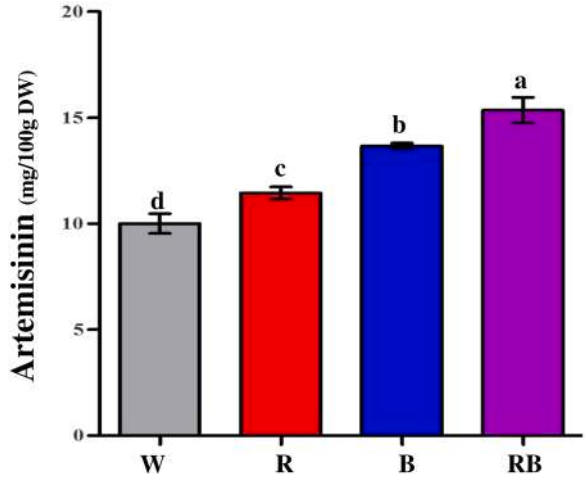

Fig. 11. The influence of varying light conditions on artemisinin production in *Artemisia annua*. The graphical bar presented the mean value with a standard error (± SE) obtained from the three independent studies (n = 3) with distinct letters that are significantly different ($P < 0.05$). One-way ANOVA was applied for data analysis.

respectively, as compared to W light.

A total of five genes involved in the biosynthetic pathway of flavonoids were also studied here using RT-PCR. The analysis of *Phenylalanine ammonia-lyase (PAL), cinnamate-4-hydroxylase (C4H), 4-coumarate CoA ligase (4CL), chalcone synthase (CHS),* and *flavonoid-3′-hydroxylase (F3′H)* was carried out in this study. By comparing different treated and control *A. annua* plants, all five genes showed significant changes in their expression. The expression values of the *PAL* gene in the shikimate pathway were observed to increment by 15.6, 15.1, and 3.9-fold under RB, B, and R light conditions compared to W light. Similarly, the expression values of the *C4H* gene increased by 5.9, 4.8, and 2.9-fold, while the *4CL* gene showed increases of 6.3, 5.4, and 1.4-fold. The *CHS* gene exhibited fold increases of 4, 2.8, and 2, and the *F3′H* gene showed increments of 4.3, 2.8, and 1.6-fold under RB, B, and R light conditions compared to W light. The Bioconductor R heatmap and gene clustering confirm that all five substantially up-regulated genes under different light conditions cluster in two groups (Fig. 13). The first group contains W and R light treatments, while the second group has B and RB light exposures.

3.10. Correlation analysis

Correlation analysis was performed using the physiological and biochemical traits of W-light-exposed plants and plants treated with different light qualities. A symbolic and significant correlation analysis has been illustrated in Fig. 10 for physiological and biochemical traits. A positive significant correlation was observed among phenol, flavonoids, lignin, and artemisinin, whereas a contrasting negative significant correlation was observed for plant height with chlorophyll, carotenoids, and Fv/Fm.

4. Discussion

The B or R LEDs facilitate plant growth and can significantly enhance plant yields, as reported by various researchers. Many medicinal plants have been studied under in-vitro conditions exposed to R and B light, such as *Lippia rotundifolia* (de Hsie et al., 2019), *Ajuga bracteosa* (Ali et al., 2019), *Fritillaria cirrhosa* (C.-C. Chen et al., 2020), and *Pfaffia glomerata* (T. D. Silva et al., 2020). In response to differential light conditions, there is still a lack of understanding regarding the various physiological processes that regulate plant growth and secondary metabolite production in *A. annua*. In the current study, after exposure

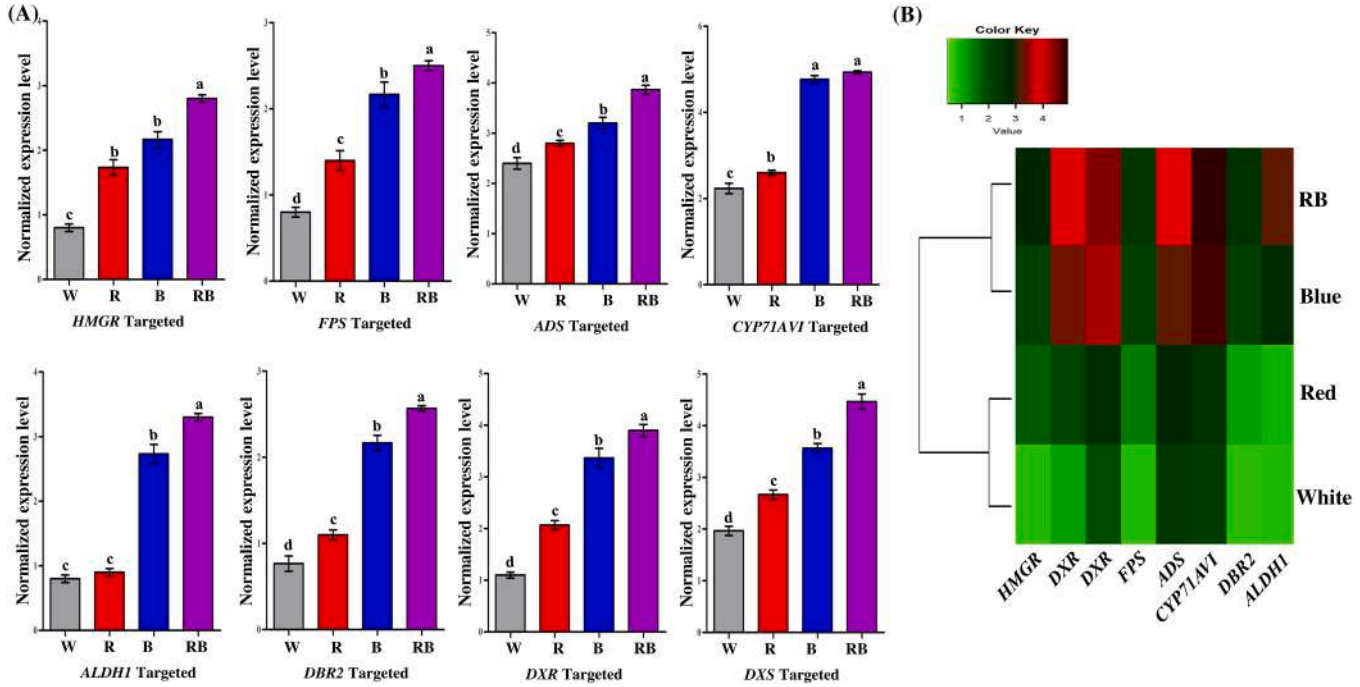

Fig. 12. RT-PCR analysis of gene expression related to the artemisinin biosynthetic pathway gene in *Artemisia annua*. Histogram depicting the normalized gene expression level as per the RT-PCR analysis and heatmap illustrating the normalized gene expression level as per the RT-PCR analysis. The presented data indicated that the mean value with a standard error (± SE) from the three independent studies (n = 3) with distinct letters is significantly different ($P < 0.05$). One-way ANOVA was applied for data analysis. A heatmap was created to represent the normalized expression levels of genes analyzed using the RT-PCR outcomes [3-Hydroxyl-3-methyglutaryl CoA reductase *(HMGR)*, 1-Deoxy-D-xylulose-5-phosphate Reductoisomerase (*DXR*), 1-Deoxy-D-xylulose-5-phosphate synthase (*DXS*), Fernasyl diphosphate synthase (*FPS*), Amorpha-4,11-diene synthase (*ADS*), Cytochrome P450 dependent monooxygenase/hydroxylase (*CYP71AVI*), Double bond reductase2 (*DBR2*), Aldehyde dehydrogenase (*ALDH1*)].

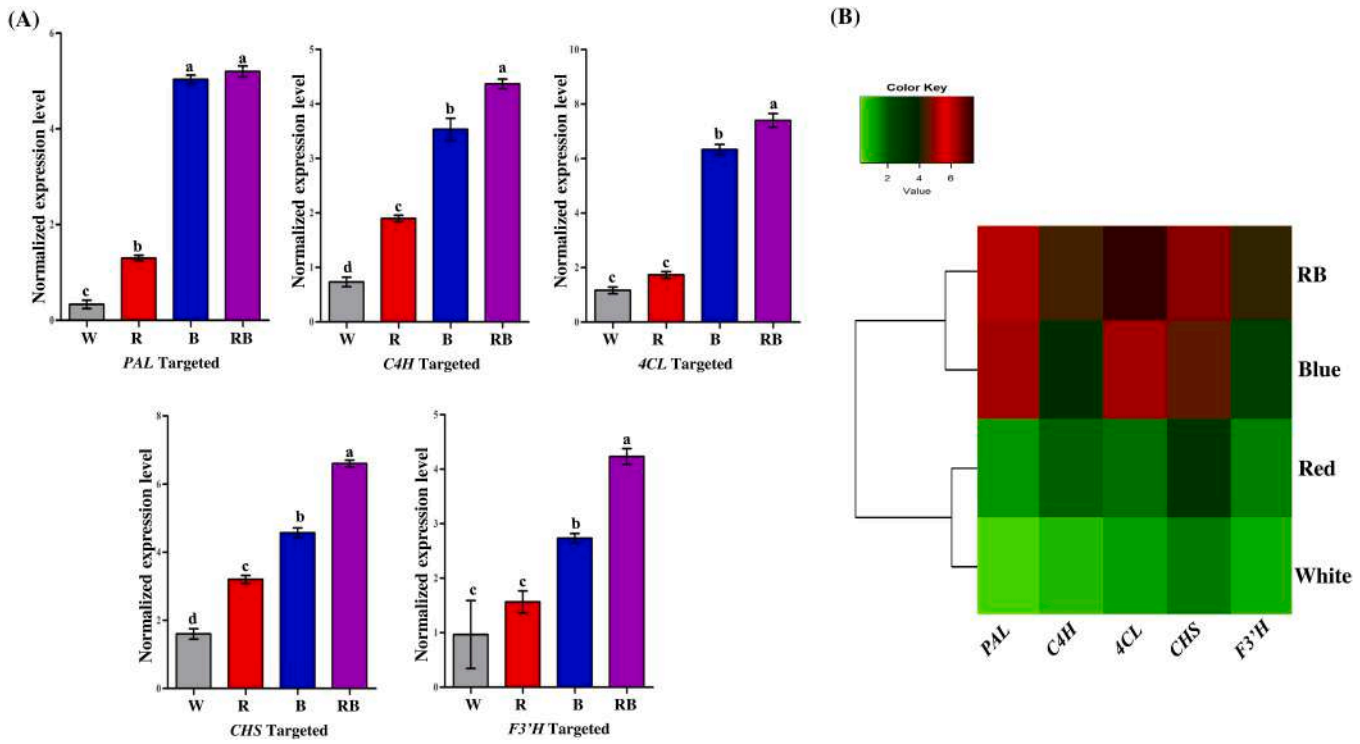

Fig. 13. RT-PCR analysis of gene expression related to the flavonoids biosynthetic pathway gene in *Artemisia annua*. Histogram depicting the normalized gene expression level as per the RT-PCR analysis and heatmap illustrating the normalized gene expression level as per the RT-PCR analysis. The presented data indicated that the mean value with a standard error (± SE) from the three independent studies (n = 3) with distinct letters is significantly different ($P < 0.05$). One-way ANOVA was applied for data analysis. A heatmap was created to represent the normalized expression levels of genes analyzed using the RT-PCR outcomes [Phenylalanine ammonia-lyase (*PAL*), Cinnamate-4-hydroxylase (*C4H*), 4-coumarate CoA ligase (*4CL*), Chalcone synthase (*CHS*), Flavonoid-3′-hydroxylase (*F3′H*)].

to different light spectra for ten days, the morphological characteristics and growth of *A. annua* showed significant changes and alterations. In our study, it can be seen that petiole length and leaf area increased under B light, followed by RB light, whereas R light led to the highest plant height in *A. annua*. Similar effects have also been reported by Zheng and Van Labeke (2017). The *Scrophularia kakudensis* plant showed that stem length increased under R light, while a shorter stem was observed under B light (Manivannan, Soundararajan, Park, and Jeong, 2021). The production of gibberellin acid in response to red light may have a regulatory role in the mechanism of shoot elongation (Arney and Mitchell, 1969). Another study concluded that prolonged exposure to B light can result in alterations to the curvature of the leaf area and stem length in lettuce and soybean plants (Dougher and Bugbee, 2001). Furthermore, it has also been observed that both parameters experience a declining trend in soybeans as the proportion of B light increases. In this study, we found that B LEDs have a greater impact on *A. annua* plant biomass production compared to W or R LEDs. Our results followed *S. kakudensis* (Manivannan et al., 2021), and *Artemisia argyi* (Su. P et al., 2023), which showed a similar impact and reported an increase in plant biomass and photosynthetic pigments under monochromatic B light. However, in Romaine lettuce (Dougher and Bugbee, 2001), under monochromatic light conditions, plant biomass has a declining trend in contrast to W light (Liu et al., 2021). It can be deduced that the impacts of light quality exhibit variability across different species.

The present study revealed that the leaf morphology of *A. annua* had alterations when plantlets were exposed to different light conditions (Fig. 2). Various studies have already demonstrated that the leaves are sensitive to light signals from their external surroundings, which are perceived through the use of special photoreceptors. Thus, variable light conditions can easily alter the characteristics of the leaves and their physiological parameters, thereby affecting plant growth and developmental processes (Park et al., 2012). In our finding, the stomatal density and leaf area were increased under monochromatic B and RB light exposures in contrast to W light. Further, the expanded leaf area is directly related to the increased absorption of light hence, accelerating the process of photosynthesis. Thus, B light exhibited the highest content of photosynthetic pigments than W and R light exposure in this study. The possibility is that the white light is not as effective at stimulating photosynthesis as the monochromatic blue light. Kurilčik, A. et al., (2008) proposed that the role of B light has significant importance in both the mechanism of chlorophyll synthesis and the maturation of chloroplasts. Hence, it can be concluded that B light exhibits a higher degree of effectiveness in stimulating the accumulation of photosynthetic pigments as compared to R light. The specific balance of colors in a white light source may not be optimal for certain plant processes or compounds. White light is not being absorbed as efficiently by the plant as the monochromatic light. This could be because the white light contains a wider range of wavelengths, some of which may not be absorbed well by the plant's pigments. It is also possible that the white light is being scattered or reflected by the plant, reducing the amount of light that is absorbed.

Stomata are responsible for supplying CO_2, which is required for the fixation of carbon by photosynthesis. The stomatal opening and conductance were also influenced by different light exposures, such as stomatal conductance, which is primarily influenced by B light. Furthermore, the ϕPSII and qP values increase under single wavelengths of B light, and the minimum value was observed in R light. (Yu and Ong, 2003) also found that plants exposed to R or yellow light exhibited lower ϕPSII and qP, which suggests that B light has a greater impact on the optimal performance of ϕPSII. Therefore, the decline in the ϕPSII under the exposure of light quality is most often associated with the depletion in qP and the efficacy of the excitation energy capacity to be absorbed by the PSII centers. It can be assumed that the reduction in qP under a single wavelength of light is due to the cytochrome b6/f complex and PSI, which is a rate-limiting reaction. Under monochromatic light treatment, the NPQ consistently increased as the energy dissipated, whereas Fv/Fm

was found to be slightly different. H. Wang et al. (2009) also reported the same observation in *Cucumis sativus*. Reduced values of Fv/Fm may be an indication of the occurrence of photo-inhibition in plants exposed to stressed environmental conditions (Maxwell & Johnson, 2000). In the current study, findings showed that the Fv/Fm values remained close to the optimal range across all treatments, thereby indicating that the plants were subjected to minimal stress under differential light exposures.

In plants, reactive oxygen species (ROS) like O^{-2} and H_2O_2 are generated through various metabolic reactions. These species are typically eliminated to prevent the excessive accumulation of ROS within the cells. Nevertheless, a disparity between ROS production and its scavenging processes is an indication of.

enhancement of the oxidative stress level (Pandey et al., 2014). The current study found that RB light conditions, then B and R light, were the ones where ROS (O^{-2} and H_2O_2) production peaked. Plants acquire antioxidant defense systems, both enzymatic and non-enzymatic, to effectively combat oxidative stress. A similar activity of antioxidant enzymes was also observed in our study under light-quality exposure in *A. annua* (Fig. 7).

Antioxidant enzymes, by catalyzing a series of processes, typically protect cells from reactive oxygen species-induced cell damage. It removes and minimizes the accumulation of ROS content in the cell (Kumari et al., 2018; Schock et al., 2023). As per the results of our study, antioxidant enzymes in *A. annua* plants exhibited significant activity under RB light, followed by B and R light. In *Rehmannia glutinosa*, under B light conditions, it was found that the maximum antioxidant enzymatic activity was exhibited in the leaves and root tissues (Manivannan et al., 2015). Dutta Gupta and Sahoo (2015) also demonstrated that B light induces intensified oxidative stress enzyme activities. The SOD enzyme dismutases the reactive free radicals into H_2O_2 and O^{-2} as a primary defense response (Gill and Tuteja, 2010); therefore, under RB, B, and R light, SOD comprises the maximum free radical scavenging potential. Following this, the produced H_2O_2 will then be removed by the activity of CAT, GPX, and H_2O_2 scavengers (Shohael et al., 2006). The above-mentioned enzymes were similarly effective under RB, B, and R light irradiations when compared with W light. Peroxidase is also a key enzyme for H_2O_2 removal and exhibits a similar pattern to the other antioxidant enzymes. Our data also supported the findings of J. Zhao et al. (2020) in *Carpesium triste* and Adil et al. (2019) in *Cinidium officinale*, where they reported that RB light enhanced the activities of oxidative stress-related enzymes.

The relevance of light quality in secondary metabolism elicitation has recently acquired prominence, mostly in medicinal plants (Alvarenga et al., 2015). There has been a lot of attention paid to how light quality has triggered a response by inducing certain secondary metabolites in plants that have medicinal purposes.

The phenolic compounds, such as flavonoids and essential oils, are widely utilized in food, cosmetics, textiles, medications, and other products, either as pure, isolated chemicals or complex mixes. The quantification of flavonoids in plant material is typically conducted using HPLC. This approach has great selectivity and accuracy. It also takes a long time and may require sample preparation. The expeditious analysis or screening of unprocessed plant material during the initial stages of production is highly significant in identifying plant material that contains adequate amounts of valuable compounds. Screening methods such as colorimetric and UV–visible spectroscopy are viable techniques. Hence, the application of Raman spectroscopy has been used in this study as a viable alternative, as it enables the precise estimation of the predominant phenolic and aromatic compounds present in unprocessed plant material (in situ) with a level of precision that meets industry standards (Buchweitz et al., 2012; Manley et al., 2006). In addition, it provides greater accuracy, information, and efficiency. *A. annua* contains significant amounts of secondary metabolites, which contribute greatly to the plant's antioxidant capacity and pharmaceutical attributes Atalla and Agarwal, 1985. Recently, different plant secondary metabolites have been successfully examined using Raman spectroscopy for quality and quantity estimations (Baranska et al., 2005a, 2005b; Schulz et al., 2005). In the current study, data were obtained directly from plant leaf tissue without destroying or isolating its components. Furthermore, within this context, various types of flavonoids, such as anthocyanin and flavone glycosides, which play a significant role in plant pigmentation to combat ROS accumulation under light-quality stress, have been detected within plant tissue (Brouillard, 1983). The current study, emphasizes an *in situ* analysis of phenolics, flavonoids, and aromatic compounds like camphor, limonene, terpene-4-ol, α pinene, 1,8-cineole, β-caryophyllene, artemisinin, kaempferol, luteolin, rutin, caffeic acid, catechin, and many more components present in the intact leaves of *A. annua* (Daferera et al. 2002; Dochow et al. 2015; Farber et al. 2019; Gierlinger and Schwanninger, 2006; Moroni et al., 2008; Pompeu et al., 2018; Shipp et al., 2017; Yixing et al., 1984). This is the first study where we hereby introduce the application of Raman spectroscopy for the detection of various secondary metabolites from in situ *A. annua* leaves, along with the advantage of the Raman quantification technique for the estimation of concentrations (Supplementary table 1).

In a study, Ballaré (2014) suggested that plants respond to light signals, which regulate the phenylpropanoid pathway, resulting in increased phytochemical biosynthesis. There are many secondary metabolites, like phenols, flavonoids, and lignin, produced by the phenylpropanoid pathway. According to Samuolienė et al. (2012) findings, flavonoids, and phenols in lettuce increased when exposed to light conditions. In our result, a biochemical assay performed for the determination of the total content of phenols and flavonoids showed markedly increased content under RB light, followed by B and R light, respectively, in contrast to W light (Fig. 5).

Additionally, in the presence of light, phenylpropanoid pathway biosynthesis for modulation of phenolic compounds is also induced due to the increased activity of PAL (Koyama et al., 2012; Rai et al., 2023), a key enzyme through which primary metabolites are catalyzed. The total phenolic content greatly increased in *A. annua* under RB, a predominately B and R light condition, which has also been confirmed by the transcriptomic data (Fig. 13). In a similar study carried out by Ali et al. (2019), the accumulation of total polyphenol contents under B light application in *Ajuga bracteosa* was observed. Furthermore, Koyama et al. (2012) reported that in plants, the expression level of genes associated with the phenylpropanoid pathway, such as *phenylalanine ammonia-lyase (PAL), chalcone synthase (CHS), chalcone isomerase (CHI), flavone-3-hydroxylase (F3′H), flavonol synthase (FLS), flavonoid-30-hydroxylase, anthocyanidin synthase (ANS), and dihydroflavonol-4 reductase (DFR),* are highly up-regulated under the effects of different light conditions. In our study, we observed similar results with induced expression levels of *PAL, CHS, 4CL, C4H*, and *F3′H* genes in *A. annua*. When R, B, and RB light conditions were used, these genes were significantly up-regulated compared to the W light. Anthocyanin is a type of flavonoid present in plants, responsible for the red, blue, and purple hues found among flowers and fruits. Many reports have claimed that B light conditions enhance the level of anthocyanin (Petrella, Metzger, Blakeslee, Nangle, and Gardner, 2017). The amount of anthocyanin elicited by exposure to both B light and UV-A was increased by 31% and 11%, respectively, while, under R light in contrast to W light, the content of anthocyanin decreased by 40% (Q. Li and Kubota, 2009). We also observed anthocyanin accumulation increasing under exposure to B light, followed by RB and R light. Moreover, a significant amount of lignin was found to be accumulated under RB and B light-grown plants (Falcioni et al., 2020). Plants under R light exposure also exhibited slightly higher levels of lignin content than control plants (Falcioni et al., 2020; C.). It has been reported that the regulation of genes associated with the biosynthesis of lignin and cellulose is influenced by the quality of light. Light stimuli can change the lignification pattern and cell wall deposition in plants (Mamedes-Rodrigues et al., 2018). The finding of Q. Wang et al. (2022) concludes that B light

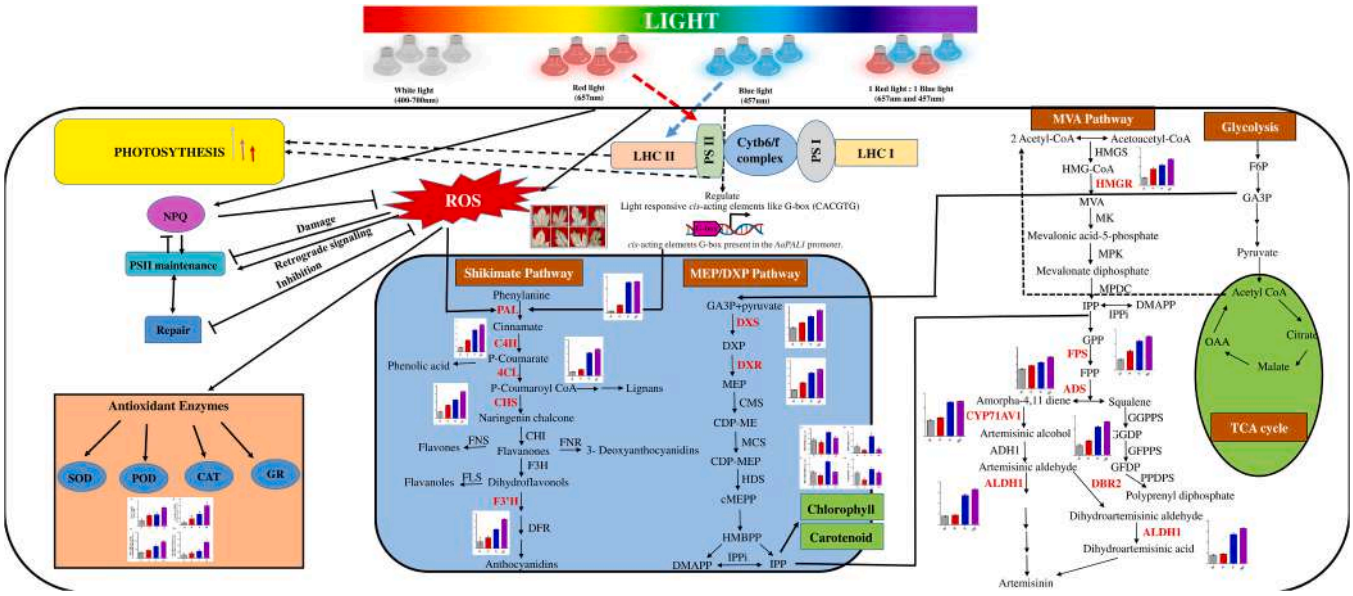

Fig. 14. Predicted model based on our results obtained showing the activated secondary metabolism, defense mechanism, and photosynthetic parameters in *Artemisia annua* L. when exposed to different light conditions. [NPQ- non-photochemical quenching, PSII-photosystem II, PSI- photosystem I, LHCI- light-harvesting complex I, LHCII- light-harvesting complex II, Cytb6/f- cytochrome b6f complex, MEP/DXP- methylerythritol phosphate pathway /1-deoxy-D-xylulose 5-phosphate, MVA- mevalonate, TCA- tricarboxylic acid cycle, SOD- superoxide dismutase, POD- peroxidase, CAT- catalase, GR- Glutathione reductase, ROS- reactive oxygen species, PAL- Phenylalanine lyase, C4H- Cinnamate-4-hydroxylase, 4CL-4-coumarate CoA ligase, CHS- Chalcone synthase, F′3 H- Flavonoid-3′-hydroxylase, DXS-1-Deoxy-D-xylulose-5-phosphate synthase, DXR-1-Deoxy-D-xylulose-5-phosphate Reductoisomerase, HMGR-3-Hydroxyl-3-methyglutaryl CoA reductase, FPS- Fernasyl diphosphate synthase, ADS- Amorpha - 4, 11-diene synthase, CYP71AV1- cytochrome P 450, ALDH1- aldehyde dehydrogenase 1, DBR2- double bond reductase 2].

enhances lignin accumulation, which is crucial for understanding the interplay of environmental controls on light qualities on lignin production. In this study, a correlation could be established between the expression levels of *PAL, C4H*, and *4CL* and the biochemical assay that measures the total phenol, flavonoid, and lignin content in *A. annua* under the quality condition.

In *A. annua*, artemisinin is biosynthesized in the subcuticular space within the glandular trichomes, which consists of ten symmetrical cells (Olofsson, Lundgren, and Brodelius, 2012), and nearly all of the biosynthetic steps for artemisinin have been identified (M. Chen et al., 2017). Briefly, four genes that are specifically expressed in trichomes (*AaADS, AaCYP71AV1, AaDBR2,* and *AaALDH1*) are responsible for converting farnesyl diphosphate (FPP) into AA or DHAA (M. Chen et al., 2017). In previous studies, it has been observed that overexpression of the TFs (transcription factors) AaTAR2 and AaMIXTA1 leads to increased production of artemisinin (Zhou et al., 2020). A novel strategy for plant breeding, improving the density of trichomes, has been suggested as a means to increase bioactive chemicals for pharmaceutical uses (Xiao, Tan, and Zhang, 2016). In this study, SEM pictures showed that leaves that were exposed to RB and B light had more glandular trichomes and were bigger than leaves that were exposed to other treatments. Surprisingly, R light has been shown to increase the density of glandular trichomes in *Alternanthera brasiliana* (Macedo, Leal-Costa, Tavares, Lage, and Esquibel, 2011). Similar results have been reported in *Olea europaea*, where the trichome density was found to be elevated under UV-B treatment in response to the defense response expressed by the plant (Liakoura et al., 1997). Our findings conclude that artemisinin levels were significantly increased under the exposure of RB light, predominantly B and R lights, respectively, and that the expression patterns of the above-mentioned key enzymes were significantly up-regulated under such treatments (Su et al., 2023). The size of trichomes increased under RB, B, and R light conditions, which can be correlated with the higher accumulation of metabolites in the glandular trichomes.

Based on the above findings and literature survey, we have tried to encapsulate the possible effects of different light spectrums on various functional mechanisms such as photosynthetic pigments, chlorophyll fluorescence parameters, ROS generation, and its mitigation strategy by *A. annua* plants via inducing antioxidant defense system and the expression of biosynthetic pathway genes. (Fig. 14). The hypothetical model here demonstrates that LHCII effectively receives B light, leading to an improvement in photosynthetic parameters similar to the effect of PSII's perception of R light. The presence of B light or a mixture of R and B light results in an increase in ROS accumulation, which consequently enhances the activity of antioxidant enzymes. Exposure to RB light, followed by monochromatic B and R lights, leads to the up-regulation of genes as compared to W light that regulates the biosynthesis pathways for the production of secondary metabolites such as artemisinin, flavonoid, phenol, anthocyanin, and lignin. Therefore, the above findings suggest that R and B LEDs and their combinations, in contrast to W light, have an impact on inducing secondary metabolite production in *A. annua*.

5. Conclusion

Being an indispensable factor, light quality directly influenced plant growth and development-associated parameters, photosynthesis, and secondary metabolism in *A. annua*. B and R LEDs influenced *A. annua* plant-enhanced photosynthetic pigment concentration and chlorophyll fluorescence parameters, including NPQ and ETR, along with antioxidant enzyme activities and secondary metabolite accumulation. Growing *A. annua* plants under RB and B light exposure is a beneficial approach for enhancing their productivity in terms of secondary metabolites. Further, we have utilized the Raman spectroscopy technique in this study for the identification of valuable secondary metabolites. From an economic perspective, this method provides an advantage in terms of cost-effectiveness. Overall, light qualities may be regarded as significant abiotic stimuli that trigger the production of plant secondary metabolites with pharmaceutically important properties, offering a promising avenue for further research and development for commercial exploitation.

Ethics approval

This work does not require ethical approval.

Funding

The authors, NR and SS, express their gratitude for the UGC non-NET research fellowship, while SK acknowledges the CSIR-SRF fellowship and PS acknowledges the UGC-JRF fellowship. This research did not receive any specific grants from funding agencies in the public, commercial, or not-for-profit sectors.

Author Statement

This research article describes the original work and has not been submitted for publication elsewhere. The consent of all the authors of this paper has been obtained for submitting the paper.

CRediT authorship contribution statement

SPR and NR established the experimental layout. NR carried out the experiments, and NR, SK, SS, and PS contributed their expertise to the written content. AKP helps in Raman spectral data analysis. The manuscript has received final approval from the SPR.

Declaration of Competing Interest

The authors declare the following financial interests/personal relationships which may be considered as potential competing interests: Prof. Shashi Pandey reports administrative support and equipment, drugs, or supplies were provided by Banaras Hindu University.

Acknowledgements

The authors would like to express their appreciation for the instrumentation facilities received from the DST-FIST and CAS Department of Botany and the Interdisciplinary School of Life Sciences (ISLS) at the Institute of Science, Banaras Hindu University, Varanasi. The authors are also grateful to the coordinator of the Institute of Eminence (IoE), BHU, for providing the necessary grant for the experimentation. We are also thankful to Prof. N.V. Chalapathi Rao for providing the SEM facility at the Department of Geology, Institute of Science, BHU, and coordinator Central Discovery Centre-DST, SATHI, BHU, for providing the Raman spectroscopy facility.

Consent to participate

The studies obtained informed consent from all individual participants.

Appendix A. Supporting information

Supplementary data associated with this article can be found in the online version at doi:10.1016/j.envexpbot.2023.105563.

References

Adil, M., Ren, X., Jeong, B.R., 2019. Light elicited growth, antioxidant enzyme activities, and production of medicinal compounds in callus culture of Cnidium officinale Makino. J. Photochem. Photobiol. B: Biol. 196, 111509 https://doi.org/10.1016/j.jphotobiol.2019.05.006.

Aebi, H., 1984. [13] Catalase in vitro. In: Methods in enzymology, Vol. 105. Elsevier, pp. 121–126. https://doi.org/10.1016/S0076-6879(84)05016-3.

Ali, H., Khan, M.A., Kayani, W.K., Dilshad, E., Rani, R., Khan, R.S., 2019. Production of biomass and medicinal metabolites through adventitious roots in Ajuga bracteosa under different spectral lights. J. Photochem. Photobiol. B: Biol. 193, 109–117. https://doi.org/10.1016/j.jphotobiol.2019.02.010.

Altangerel, N., Ariunbold, G.O., Gorman, C., Alkahtani, M.H., Borrego, E.J., Bohlmeyer, D., Scully, M.O., 2017. In vivo diagnostics of early abiotic plant stress response via Raman spectroscopy. Proc. Natl. Acad. Sci. USA 114 (13), 3393–3396. https://doi.org/10.1073/pnas.1701328114.

Altonen, B.L., Arreglado, T.M., Leroux, O., Murray-Ramcharan, M., Engdahl, R., 2020. Characteristics, comorbidities and survival analysis of young adults hospitalized with COVID-19 in New York City. PLoS One 15 (12), e0243343. https://doi.org/10.1371/journal.pone.0243343.

Alvarenga, I.C.A., Pacheco, F.V., Silva, S.T., Bertolucci, S.K.V., Pinto, J.E.B.P., 2015. In vitro culture of Achillea millefolium L.: quality and intensity of light on growth and production of volatiles. Plant Cell, Tissue Organ Cult. 122, 299–308. https://doi.org/10.1007/s11240-015-0766-7.

Apoorva, Jaiswal, D., Pandey-Rai, S., Agrawal, S.B., 2021. Untangling the UV-B radiation-induced transcriptional network regulating plant morphogenesis and secondary metabolite production. Environ. Exp. Bot. 192, 104655 https://doi.org/10.1016/j.envexpbot.2021.104655.

Arney, S.E., Mitchell, D.L., 1969. The effect of abscisic acid on stem elongation and correlative inhibition. N. Phytol. 68, 1001–1015. https://doi.org/10.1111/j.1469-8137.1969.tb06500.x.

Atalla, R.H., Agarwal, U.P., 1985. Raman microprobe evidence for lignin orientation in the cell walls of native woody tissue. Science 227 (4687), 636–638. https://doi.org/10.1126/science.227.4687.636.

Ballaré, C.L., 2014. Light regulation of plant defense. Annu. Rev. Plant Biol. 65, 335–363. https://doi.org/10.1146/annurev-arplant-050213-040145.

Baranska, M., Schulz, H., Baranski, R., Nothnagel, T., Christensen, L.P., 2005a. In situ simultaneous analysis of polyacetylenes, carotenoids and polysaccharides in carrot roots. J. Agric. Food Chem. 53 (17), 6565–6571. https://doi.org/10.1007/s00425-005-1566-9.

Baranska, M., Schulz, H., Siuda, R., Strehle, M., Rösch, P., Popp, J., Manley, M., 2005b. Quality control of Harpagophytum procumbens and its related phytopharmaceutical products by means of NIR-FT-Raman spectroscopy. Biopolym.: Orig. Res. Biomol. 77 (1), 1–8. https://doi.org/10.1021/jf0510440.

Beauchamp, C., Fridovich, I., 1971. Superoxide dismutase: improved assays and an assay applicable to acrylamide gels. Anal. Biochem. 44 (1), 276–287. https://doi.org/10.1016/0003-2697(71)90370-8.

Britton, C., Mehley, A., 1955. Assay of catalase and peroxidase. Methods Enzymol. 2, 764–775. https://doi.org/10.1016/S0076-6879(55)02300-8.

Brouillard, R., 1983. The in vivo expression of anthocyanin colour in plants. Phytochemistry 22 (6), 1311–1323. https://doi.org/10.1016/S0031-9422(00)84008-X.

Buchweitz, M., Gudi, G., Carle, R., Kammerer, D.R., Schulz, H., 2012. Systematic investigations of anthocyanin–metal interactions by Raman spectroscopy. J. Raman Spectrosc. 43 (12), 2001–2007. https://doi.org/10.1002/jrs.4123.

Casal, J.J., 2013. Photoreceptor signaling networks in plant responses to shade. Annu. Rev. Plant Biol. 64, 403–427. https://doi.org/10.1146/annurev-arplant-050312-120221.

Chang, C.-C., Yang, M.-H., Wen, H.-M., Chern, J.-C., 2002. Estimation of total flavonoid content in propolis by two complementary colorimetric methods. J. Food Drug Anal. 10 (3) https://doi.org/10.38212/2224-6614.2748.

Chen, C.-C., Lee, M.-R., Wu, C.-R., Ke, H.-J., Xie, H.-M., Tsay, H.-S., Chang, H.-C., 2020. LED lights affecting morphogenesis and isosteroidal alkaloid contents in Fritillaria cirrhosa D. Don—an important Chinese medicinal herb. Plants 9 (10), 1351. https://doi.org/10.3390/plants9101351.

Chen, M., Yan, T., Shen, Q., Lu, X., Pan, Q., Huang, Y., Jiang, W., 2017. GLANDULAR TRICHOME-SPECIFIC WRKY 1 promotes artemisinin biosynthesis in Artemisia annua. N. Phytol. 214 (1), 304–316. https://doi.org/10.1111/nph.14373.

Daferera, D.J., Tarantilis, P.A., Polissiou, M.G., 2002. Characterization of essential oils from Lamiaceae species by Fourier transform Raman spectroscopy. J. Agric. Food Chem. 50 (20), 5503–5507. https://doi.org/10.1021/jf0203489.

Dhaka, R.K., Sinha, S.K., Gunaga, R.P., Thakur, N.S., 2019. Modification in protocol for estimation of Klason-lignin content by gravimetric method. IJCS 7 (5), 2661–2664. https://doi.org/10.13140/RG.2.2.10316.77443.

Dochow, S., Ma, D., Latka, I., Bocklitz, T., Hartl, B., Bec, J., Popp, J., 2015. Combined fiber probe for fluorescence lifetime and Raman spectroscopy. Anal. Bioanal. Chem. 407, 8291–8301. https://doi.org/10.1007/s00216-015-8800-5.

Donato, R., Santomauro, F., Bilia, A.R., Flamini, G., Sacco, C., 2015. Antibacterial activity of Tuscan Artemisia annua essential oil and its major components against some foodborne pathogens. LWT-Food Sci. Technol. 64 (2), 1251–1254. https://doi.org/10.1016/j.lwt.2015.07.014.

Dougher, T.A., Bugbee, B., 2001. Differences in the Response of Wheat, Soybean and Lettuce to Reduced Blue Radiation¶. Photochem. Photobiol. 73 (2), 199–207. https://doi.org/10.1562/0031-8655(2001)0730199DITROW2.0.CO2.

Dutta Gupta, S., Sahoo, T., 2015. Light emitting diode (LED)-induced alteration of oxidative events during in vitro shoot organogenesis of Curculigo orchioides Gaertn. Acta Physiol. Plant. 37, 1–9. https://doi.org/10.1007/s11738-015-1990-9.

Falcioni, R., Moriwaki, T., Perez-Llorca, M., Munné-Bosch, S., Gibin, M.S., Sato, F., Rüggeberg, M., 2020. Cell wall structure and composition is affected by light quality in tomato seedlings. J. Photochem. Photobiol. B: Biol. 203, 111745 https://doi.org/10.1016/j.jphotobiol.2019.111745.

Farber, C., Shires, M., Ong, K., Byrne, D., Kurouski, D., 2019. Raman spectroscopy as an early detection tool for rose rosette infection. Planta 250, 1247–1254. https://doi.org/10.1007/s00425-019-03216-0.

Galvão, V.C., Fankhauser, C., 2015. Sensing the light environment in plants: photoreceptors and early signaling steps. Curr. Opin. Neurobiol. 34, 46–53. https://doi.org/10.1016/j.conb.2015.01.013.

Gam, D.T., Khoi, P.H., Ngoc, P.B., Linh, L.K., Hung, N.K., Anh, P.T.L., Ha, C.H., 2020. LED lights promote growth and flavonoid accumulation of Anoectochilus roxburghii and are linked to the enhanced expression of several related genes. Plants 9 (10), 1344. https://doi.org/10.3390/plants9101344.

Ghasemzadeh, A., Jaafar, H.Z., Rahmat, A., 2010. Synthesis of phenolics and flavonoids in ginger (Zingiber officinale Roscoe) and their effects on photosynthesis rate. Int. J. Mol. Sci. 11 (11), 4539–4555. https://doi.org/10.3390/ijms11114539.

Gierlinger, N., Schwanninger, M., 2006. Chemical imaging of poplar wood cell walls by confocal Raman microscopy. Plant Physiol. 140 (4), 1246–1254. https://doi.org/10.1104/pp.105.066993.

Gill, S.S., Tuteja, N., 2010. Reactive oxygen species and antioxidant machinery in abiotic stress tolerance in crop plants. Plant Physiol. Biochem. 48 (12), 909–930. https://doi.org/10.1016/j.plaphy.2010.08.016.

Goins, G.D., Ruffe, L.M., Cranston, N.A., Yorio, N.C., Wheeler, R.M., Sager, J.C., 2001. *Salad crop production under different wavelengths of red light-emitting diodes (LEDs)* (0148-7191). Retrieved. https://doi.org/10.4271/2001-01-2422.

Hess, W., 1966. Fixation and staining of fungus hyphae and host plant root tissues for electron microscopy. Stain Technol. 41 (1), 27–35. https://doi.org/10.3109/10520296609116276.

Hoagland, D.R., & Arnon, D.I. (1950). The water-culture method for growing plants without soil. *Circular. California agricultural experiment station, 347* (2nd edit).

Hou, H.-Y., Yang, X., Mao, Z.-L., Yao, X.-Y., Chen, X.-B., 2019. Raman study of impurity influence on active center in artemisinin. Spectrochim. Acta Part A: Mol. Biomol. Spectrosc. 221, 117206 https://doi.org/10.1016/j.saa.2019.117206.

de Hsie, B.S., Bueno, A.I.S., Bertolucci, S.K.V., de Carvalho, A.A., da Cunha, S.H.B., Martins, E.R., Pinto, J.E.B.P., 2019. Study of the influence of wavelengths and intensities of LEDs on the growth, photosynthetic pigment, and volatile compounds production of Lippia rotundifolia Cham in vitro. J. Photochem. Photobiol. B: Biol. 198, 111577 https://doi.org/10.1016/j.jphotobiol.2019.111577.

Huché-Thélier, L., Crespel, L., Le Gourrierec, J., Morel, P., Sakr, S., Leduc, N., 2016. Light signaling and plant responses to blue and UV radiations—Perspectives for applications in horticulture. Environ. Exp. Bot. 121, 22–38. https://doi.org/10.1016/j.envexpbot.2015.06.009.

Imeh, U., Khokhar, S., 2002. Distribution of conjugated and free phenols in fruits: antioxidant activity and cultivar variations. J. Agric. Food Chem. 50 (22), 6301–6306. https://doi.org/10.1021/jf020342j.

Koyama, K., Ikeda, H., Poudel, P.R., Goto-Yamamoto, N., 2012. Light quality affects flavonoid biosynthesis in young berries of Cabernet Sauvignon grape. Phytochemistry 78, 54–64. https://doi.org/10.1016/j.phytochem.2012.02.026.

Kumari, A., Pandey, N., Pandey-Rai, S., 2018. Exogenous salicylic acid-mediated modulation of arsenic stress tolerance with enhanced accumulation of secondary metabolites and improved size of glandular trichomes in Artemisia annua L. Protoplasma 255, 139–152. https://doi.org/10.1007/s00709-017-1136-6.

Kurilčik, A., Miklušytė-Čanova, R., Dapkūnienė, S., Žilinskaitė, S., Kurilčik, G., Tamulaitis, G., Žukauskas, A., 2008. In vitro culture of Chrysanthemum plantlets using light-emitting diodes. Cent. Eur. J. Biol. 3, 161–167. https://doi.org/10.2478/s11535-008-0006-9.

Lalani, M., Kitutu, F.E., Clarke, S.E., Kaur, H., 2017. Anti-malarial medicine quality field studies and surveys: a systematic review of screening technologies used and reporting of findings. Malar. J. 16 (1), 1–14. https://doi.org/10.1186/s12936-017-1852-6.

Lazzarini, L.E.S., Bertolucci, S.K.V., Pacheco, F.V., dos Santos, J., Silva, S.T., de Carvalho, A.A., Pinto, J.E.B.P., 2018. Quality and intensity of light affect Lippia gracilis Schauer plant growth and volatile compounds in vitro. Plant Cell, Tissue Organ Cult. (PCTOC) 135, 367–379. https://doi.org/10.1007/s11240-018-1470-1.

Li, A., Li, S., Wu, X., Zhang, J., He, A., Zhao, G., Yang, X., 2016. Effect of light intensity on leaf photosynthetic characteristics and accumulation of flavonoids in Lithocarpus litseifolius (Hance) Chun.(Fagaceae). Open J. For. 6 (5), 445–459. https://doi.org/10.4236/ojf.2016.65034.

Li, Q., Kubota, C., 2009. Effects of supplemental light quality on growth and phytochemicals of baby leaf lettuce. Environ. Exp. Bot. 67 (1), 59–64. https://doi.org/10.1016/j.envexpbot.2009.06.011.

Liakoura, V., Stefanou, M., Manetas, Y., Cholevas, C., Karabourniotis, G., 1997. Trichome density and its UV-B protective potential are affected by shading and leaf position on the canopy. Environ. Exp. Bot. 38 (3), 223–229. https://doi.org/10.1016/S0098-8472(97)00005-1.

Liu, B., Long, H., Yan, J., Ye, L., Zhang, Q., Chen, H., Sun, S., 2021. A HY5–COL3–COL13 regulatory chain for controlling hypocotyl elongation in Arabidopsis. Plant, Cell Environ. 44 (1), 130–142. https://doi.org/10.1111/pce.13899.

Macedo, A.F., Leal-Costa, M.V., Tavares, E.S., Lage, C.L.S., Esquibel, M.A., 2011. The effect of light quality on leaf production and development of in vitro-cultured plants of Alternanthera brasiliana Kuntze. Environ. Exp. Bot. 70 (1), 43–50. https://doi.org/10.1016/j.envexpbot.2010.05.012.

Mancinelli, A., Yang, C.-P.H., Lindquist, P., Anderson, O., Rabino, I., 1975. Photocontrol of anthocyanin synthesis: III. The action of streptomycin on the synthesis of chlorophyll and anthocyanin. Plant Physiol. 55 (2), 251–257. https://doi.org/10.1104/pp.55.2.251.

Manivannan, A., Soundararajan, P., Park, Y.G., Jeong, B.R., 2021. Physiological and proteomic insights into red and blue light-mediated enhancement of in vitro growth in Scrophularia kakudensis—A potential medicinal plant. Front. Plant Sci. 11, 607007 https://doi.org/10.3389/fpls.2020.607007.

Manley, M., Joubert, E., Botha, M., 2006. Quantification of the major phenolic compounds, soluble solid content and total antioxidant activity of green rooibos (Aspalathus linearis) by means of near infrared spectroscopy. J. Infrared Spectrosc. 14 (4), 213–222. https://doi.org/10.1255/jnirs.638.

Mirbehbahani, F.S., Hejazi, F., Najmoddin, N., Asefnejad, A., 2020. Artemisia annua L. as a promising medicinal plant for powerful wound healing applications. Prog. Biomater. 9, 139–151. https://doi.org/10.1007/s40204-020-00138-z.

Miyagi, A., Uchimiya, H., Kawai-Yamada, M., 2017. Synergistic effects of light quality, carbon dioxide and nutrients on metabolite compositions of head lettuce under artificial growth conditions mimicking a plant factory. Food Chem. 218, 561–568. https://doi.org/10.1016/j.foodchem.2016.09.102.

Monostori, I., Heilmann, M., Kocsy, G., Rakszegi, M., Ahres, M., Altenbach, S.B., Simon-Sarkadi, L., 2018. LED lighting–modification of growth, metabolism, yield and flour composition in wheat by spectral quality and intensity. Front. Plant Sci. 9, 605 https://doi.org/10.3389/fpls.2018.00605.

Moroni, L., Gellini, C., Miranda, M.M., Salvi, P.R., Foresti, M.L., Innocenti, M.,. & Salvietti, E. (2008). Raman and infrared characterization of the vibrational properties of the antimalarial drug artemisinin. https://doi.org/10.1002/jrs.1880.

Neff, M.M., Fankhauser, C., Chory, J., 2000. Light: an indicator of time and place. Genes Dev. 14 (3), 257–271. https://doi.org/10.1101/gad.14.3.257.

Olle, M., Viršile, A., 2013. The effects of light-emitting diode lighting on greenhouse plant growth and quality. Agric. Food Sci. 22 (2), 223–234. https://doi.org/10.23986/afsci.7897.

Olofsson, L., Lundgren, A., Brodelius, P.E., 2012. Trichome isolation with and without fixation using laser microdissection and pressure catapulting followed by RNA amplification: expression of genes of terpene metabolism in apical and sub-apical trichome cells of Artemisia annua L. Plant Sci. 183, 9–13. https://doi.org/10.1016/j.plantsci.2011.10.019.

Pandey, N., Pandey-Rai, S., 2014. Short term UV-B radiation-mediated transcriptional responses and altered secondary metabolism of in vitro propagated plantlets of Artemisia annua L. Plant Cell, Tissue Organ Cult. (PCTOC) 116, 371–385. https://doi.org/10.1007/s11240-013-0413-0.

Pandey, N., Meena, R.P., Rai, S.K., Pandey-Rai, S., 2016. In vitro generation of high artemisinin yielding salt tolerant somaclonal variant and development of SCAR marker in Artemisia annua L. Plant Cell, Tissue Organ Cult. (PCTOC) 127, 301–314. https://doi.org/10.1007/s11240-016-1050-1.

Park, Y.G., Park, J.E., Hwang, S.J., Jeong, B.R., 2012. Light source and CO 2 concentration affect growth and anthocyanin content of lettuce under controlled environment. Hortic., Environ., Biotechnol. 53, 460–466. https://doi.org/10.1007/s13580-012-0821-9.

Petrella, D.P., Metzger, J.D., Blakeslee, J.J., Nangle, E.J., Gardner, D.S., 2017. Effects of blue light and phenotype on anthocyanin accumulation in accessions and cultivars of rough bluegrass. Crop Sci. 57 (S1), S-209–S-217. https://doi.org/10.2135/cropsci2016.05.0438.

Pompeu, D.R., Larondelle, Y., Rogez, H., Abbas, O., Pierna, J.A.F., Baeten, V., 2018. Characterization and discrimination of phenolic compounds using Fourier transform Raman spectroscopy and chemometric tools. Base. https://doi.org/10.25518/1780-4507.16270.

Porra, R., Thompson, W. a A., Kriedemann, P., 1989. Determination of accurate extinction coefficients and simultaneous equations for assaying chlorophylls a and b extracted with four different solvents: verification of the concentration of chlorophyll standards by atomic absorption spectroscopy. Biochim. Et Biophys. Acta (BBA)-Bioenerget. 975 (3), 384–394. https://doi.org/10.1016/S0005-2728(89)80347-0.

Rai, N., Kumari, S., Singh, S., Saha, P., Pandey-Rai, S., 2023. Genome-wide identification of bZIP transcription factor family in Artemisia annua, its transcriptional profiling and regulatory role in phenylpropanoid metabolism under different light conditions. Physiol. Mol. Biol. Plants 29 (7), 905–925. https://doi.org/10.1007/s12298-023-01338-0.

Rao, M.V., Davis, K.R., 1999. Ozone-induced cell death occurs via two distinct mechanisms in Arabidopsis: the role of salicylic acid. Plant J. 17 (6), 603–614. https://doi.org/10.1046/j.1365-313X.1999.00400.x.

Samuolienė, G., Sirtautas, R., Brazaitytė, A., Viršilė, A., Duchovskis, P., 2012. Supplementary red-LED lighting and the changes in phytochemical content of two baby leaf lettuce varieties during three seasons. J. Food Agric. Environ. 10 (3–4), 701–706. https://doi.org/10.1234/4.2012.3491.

Sanja, C., Milka, M., Danijiela, V., Adisa, P., 2012. Chemical composition and antioxidant and antimicrobial activity of essential oil of Artemisia annual L. from Bosnia. Ind. Crop. Prod. 37, 479–485. https://doi.org/10.1016/j.indcrop.2011.07.024.

Schaedle, M., Bassham, J.A., 1977. Chloroplast glutathione reductase. Plant Physiol. 59 (5), 1011–1012. https://doi.org/10.1104/pp.59.5.1011.

E.N. Schock J.R. York C. LaBonne The developmental and evolutionary origins of cellular pluripotency in the vertebrate neural crest Pap. Presente Semin. Cell Dev. Biol. 2023 doi: 10.1016/j.semcdb.2022.04.008.

Schulz, H., Baranska, M., Quilitzsch, R., Schütze, W., Lösing, G., 2005. Characterization of peppercorn, pepper oil, and pepper oleoresin by vibrational spectroscopy methods. J. Agric. Food Chem. 53 (9), 3358–3363. https://doi.org/10.1021/jf048137m.

Shipp, D.W., Sinjab, F., Notingher, I., 2017. Raman spectroscopy: techniques and applications in the life sciences. Adv. Opt. Photonics 9 (2), 315–428. https://doi.org/10.1364/AOP.9.000315.

Shohael, A., Ali, M., Yu, K., Hahn, E., Islam, R., Paek, K., 2006. Effect of light on oxidative stress, secondary metabolites and induction of antioxidant enzymes in Eleutherococcus senticosus somatic embryos in bioreactor. Process Biochem. 41 (5), 1179–1185. https://doi.org/10.1016/j.procbio.2005.12.015.

Silva, S.T., Bertolucci, S.K.V., da Cunha, S.H.B., Lazzarini, L.E.S., Tavares, M.C., Pinto, J. E.B.P., 2017. Effect of light and natural ventilation systems on the growth parameters and carvacrol content in the in vitro cultures of Plectranthus amboinicus (Lour.) Spreng. Plant Cell, Tissue Organ Cult. (PCTOC) 129, 501–510. https://doi.org/10.1007/s11240-017-1195-6.

Silva, T.D., Batista, D.S., Fortini, E.A., de Castro, K.M., Felipe, S.H.S., Fernandes, A.M., de Freitas Correia, L.N., 2020. Blue and red light affects morphogenesis and 20-hydroxyecdisone content of in vitro Pfaffia glomerata accessions. J. Photochem. Photobiol. B: Biol. 203, 111761 https://doi.org/10.1016/j.jphotobiol.2019.111761.

Singh, S., Saha, P., Rai, N., Kumari, S., Pandey-Rai, S., 2023. Unravelling triterpenoid biosynthesis in plants for applications in bioengineering and large-scale sustainable production. Ind. Crops Prod. 199, 116789 https://doi.org/10.1016/j.indcrop.2023.116789.

Su, P., Ding, S., Wang, D., Kan, W., Yuan, M., Chen, X., Wu, L., 2023. Plant morphology, secondary metabolites and chlorophyll fluorescence of Artemisia argyi under different LED environments. Photosynth. Res. 1–12. https://doi.org/10.1007/s11120-023-01026-w.

Thordal-Christensen, H., Zhang, Z., Wei, Y., Collinge, D.B., 1997. Subcellular localization of H2O2 in plants. H2O2 accumulation in papillae and hypersensitive response during the barley—powdery mildew interaction. Plant J. 11 (6), 1187–1194. https://doi.org/10.1046/j.1365-313X.1997.11061187.x.

Wang, H., Gu, M., Cui, J., Shi, K., Zhou, Y., Yu, J., 2009. Effects of light quality on CO_2 assimilation, chlorophyll-fluorescence quenching, expression of Calvin cycle genes and carbohydrate accumulation in Cucumis sativus. J. Photochem. Photobiol. B: Biol. 96 (1), 30–37. https://doi.org/10.1016/j.jphotobiol.2009.03.010.

Wang, Q., Gong, X., Xie, Z., Qi, K., Yuan, K., Jiao, Y., Tao, S., 2022. Cryptochrome-mediated blue-light signal contributes to lignin biosynthesis in stone cells in pear fruit. Plant Sci. 318, 111211 https://doi.org/10.1016/j.plantsci.2022.111211.

Xiao, L., Tan, H., Zhang, L., 2016. Artemisia annua glandular secretory trichomes: the biofactory of antimalarial agent artemisinin. Sci. Bull. 61 (1), 26–36. https://doi.org/10.1007/s11434-015-0980-z.

Yang, X., Xu, H., Shao, L., Li, T., Wang, Y., Wang, R., 2018. Response of photosynthetic capacity of tomato leaves to different LED light wavelength. Environ. Exp. Bot. 150, 161–171. https://doi.org/10.1016/j.envexpbot.2018.03.013.

Yang, Z., He, W., Mou, S., Wang, X., Chen, D., Hu, X., Bai, J., 2017. Plant growth and development of pepper seedlings under different photoperiods and photon flux ratios of red and blue LEDs. Trans. Chin. Soc. Agric. Eng. 33 (17), 173–180. https://doi.org/10.11975/j.issn.1002-6819.2017.17.023.

Yixing, F., Ziying, Z., Dajun, H., 1984. Conformation of the vibrational frequency of peroxide group in arteannuin and related compounds. Acta Chim. Sin. 42 (12), 1312.

Yu, H., Ong, B.-L., 2003. Effect of radiation quality on growth and photosynthesis of Acacia mangium seedlings. Photosynthetica 41, 349–355. https://doi.org/10.1023/B:PHOT.0000015458.11643.b2.

Yuan, M., Jia, X., Ding, C., Zeng, H., Du, L., Yuan, S., Liu, J., 2015. Effect of fluorescence light on phenolic compounds and antioxidant activities of soybeans (Glycine max L. Merrill) during germination. Food Sci. Biotechnol. 24, 1859–1865. https://doi.org/10.1007/s10068-015-0243-4.

Zhang, X.-H., Zheng, X.-T., Sun, B.-Y., Peng, C.-L., Chow, W.S., 2018. Over-expression of the CHS gene enhances resistance of Arabidopsis leaves to high light. Environ. Exp. Bot. 154, 33–43. https://doi.org/10.1016/j.envexpbot.2017.12.011.

Zhao, J., Thi, L.T., Park, Y.G., Jeong, B.R., 2020. Light quality affects growth and physiology of Carpesium triste maxim. cultured in vitro. Agriculture 10 (7), 258. https://doi.org/10.3390/agriculture10070258.

Zhao, S.-S., Zeng, M.-Y., 1985. Spektrometrische hochdruck-flüssigkeits-chromatographische (HPLC) Untersuchungen zur Analytik von Qinghaosu. Planta Med. 51 (03), 233–237. https://doi.org/10.1055/s-2007-969466.

Zheng, L., Van Labeke, M.-C., 2017. Long-term effects of red-and blue-light emitting diodes on leaf anatomy and photosynthetic efficiency of three ornamental pot plants. Front. Plant Sci. 8, 917 https://doi.org/10.3389/fpls.2017.00917.

Zhou, Z., Tan, H., Li, Q., Li, Q., Wang, Y., Bu, Q., Zhang, L., 2020. TRICHOME AND ARTEMISININ REGULATOR 2 positively regulates trichome development and artemisinin biosynthesis in Artemisia annua. N. Phytol. 228 (3), 932–945. https://doi.org/10.1111/nph.16777.